CHAPTER

Optical performance monitoring of optical phase–modulated signals 12

Bartłomiej Kozicki
NTT Network Innovation Laboratories, NTT Corporation, Japan

12.1 INTRODUCTION

The continuing growth of the traffic volume generated by broadband Internet connections, distributed storage services, or cloud/grid computing is placing a rising demand on network operators to provide increasing amounts of bandwidth. This is expected to occur without significant changes in pricing of the services, which forces network operators to look for novel solutions in the field of optical transport networks. In order to take advantage of the available resources efficiently, the envisaged transparent optical network will accommodate dense wavelength-division-multiplexed (DWDM), high–bit rate channels.[1] Consequently, the currently dominating on-off keying (OOK) modulation formats will pose a challenge due to limited tolerance toward chromatic dispersion (CD) and nonlinear distortions, as well as relatively low receiver sensitivity, which constrict the network design to a small number of transparent nodes.[2] The solution lies in the adaptation of advanced modulation formats that, in the context of optical modulation, relate to all formats beyond binary intensity modulation.[3] Advances in high-speed transponder electronics techniques such as controlled signal predistortion, maximum-likelihood sequence estimation (MLSE), and forward error correction (FEC) made increases in bit rates of individual channels possible.[3–5] More importantly, the introduction of binary and multilevel phase modulation gave the opportunity to develop formats with high spectral efficiency (SE) and receiver sensitivity.[6]

As a result, a number of modulation formats have been introduced to the optical communication systems. In particular, phase-modulation formats have gained renewed interest in optical domain in the context of differential encoding and balanced detection.[7,8] The return-to-zero differential phase-shift keying (RZ-DPSK) modulation provides an approximately 3-dB receiver sensitivity advantage when compared to RZ-OOK, as shown in Figure 12.1(a). It has been reported that the DPSK modulation formats can tolerate larger amounts of polarization mode dispersion (PMD) than OOK systems in both compensated and uncompensated systems.[9] The RZ-DPSK format provides resilience to narrow optical filtering[8] and crossphase modulation (XPM) both in fiber[10,11] and in semiconductor optical amplifiers.[12] Spectral efficiency of 0.4 bit/s/Hz in the RZ-DPSK format can be further enhanced by alternate phase modulation of intense RZ pulses, thereby forming the carrier-suppressed RZ-DPSK (CSRZ-DPSK) format.[13] The CSRZ-DPSK format has been shown to allow transmission with SE of up to 0.8 bit/s/Hz.[14,15] Similarly, high SE has been achieved with multilevel phase modulation. The return-to-zero, differential quadrature phase-shift keying (RZ-DQPSK) signal occupies

Doi: 10.1016/B978-0-12-374950-5.00012-2

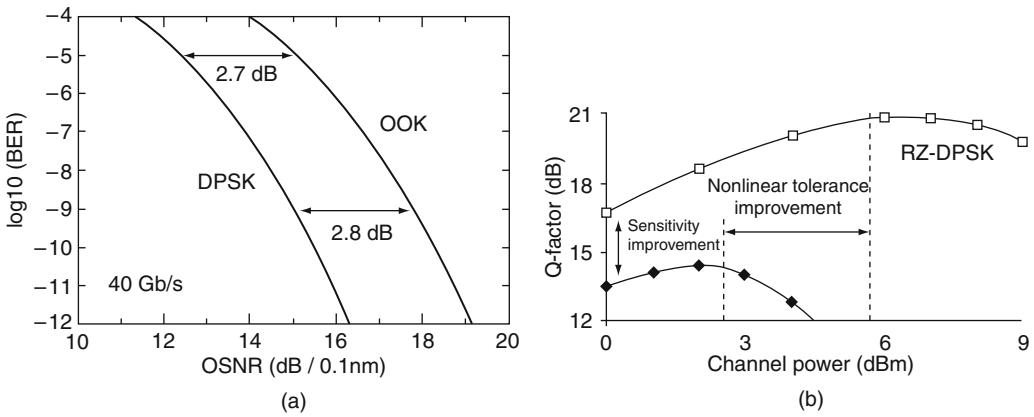

FIGURE 12.1

(a) Comparison of required OSNR between DPSK and OOK formats. (b) Comparison of nonlinear tolerance between RZ-DPSK and RZ-OOK formats.[6,7]

only 50% of the bandwidth of an RZ-DPSK signal at the same bit rate.[16] The DQPSK format has also been shown to provide better linear performance than other quaternary formats, such as differential phase-amplitude-shift keying (DPASK).[17,18] This is achieved through encoding 2 bits in four phase states of one symbol. The format relaxes the requirement for high-speed modulator electronics, the compressed spectrum ensures resilience to CD, and the longer symbol duration compared to the binary modulation makes DQPSK more robust to PMD. In conjunction with polarization multiplexing (PolMux), the RZ-DQPSK format can achieve SE of up to 1.6 bit/s/Hz.[6] The multilevel encoding of RZ-DQPSK results in an approximately 1-dB receiver sensitivity penalty when compared to the RZ-DPSK format.[19] Nevertheless, the high SE of the RZ-DQPSK and the receiver sensitivity advantage of the RZ-DPSK make these formats an attractive solution for transparent transmission.

Multilevel modulation formats exceeding four levels have also been explored both in simulation and experiment. Formats like ASK-DPSK, 8DPSK, 16-quadrature amplitude modulation (16-QAM), and 64-QAM promise even higher SE. However, the increase in the number of bits per symbol results in a reduction of the distance between the signal points in the constellation map, which in turn causes degradation of receiver sensitivity, as well as increases the impact of CD and PMD.[20–22]

12.2 PERFORMANCE OF PHASE-MODULATED SIGNALS

The use of phase modulation in optical communication systems is not a new concept, as the phase-modulated systems had been studied in the context of single-span transmission with coherent detection before development of the erbium-doped fiber amplifiers (EDFAs).[23] The deployment of DPSK in optical transmission systems is advantageous from several viewpoints. In a linear channel dominated by the amplified spontaneous emission (ASE) noise, the DPSK signal demonstrates the same level of bit error ratio (BER) at an OSNR 3-dB lower compared to the OOK when balanced detection is used.

The decrease of required OSNR is not the only advantage of the DPSK system. The RZ-DPSK format also shows improved performance during transmission through a nonlinear channel especially in the context of reduced XPM influence, as can be observed in Figure 12.1(b). In RZ-DPSK transmission, all bits have the same pulse power. In addition, in the case of pulse-overlapped 40-Gb/s transmission, the DPSK format is found to undergo less overall nonlinear penalty than OOK.[6] The influence of intrachannel four-wave mixing (iFWM) on the phase-modulated format is lower with the same average power due to the lower peak power and the correlation of nonlinear phase shifts between any two neighboring bits. The RZ-DPSK format has been shown to be more robust than OOK to narrowband filtering.[24] Further improvements in filtering performance are achieved in the multilevel RZ-DQPSK signal, which occupies 50% of the spectrum of the RZ-DPSK signal generated at the same bit rate. The compressed spectrum allows achieving high SE in DWDM systems and high tolerance to CD. Longer bit duration, compared to the binary modulation, also makes the DQPSK more robust against PMD.[19]

12.2.1 Signal impairments

Transmission of signals in a transparent domain results in the accumulation of optical impairments. The impairments degrade the quality of the signal at the receiver, leading to reception errors. This section describes the most crucial optical phenomena that influence the performance of phase-modulated channels.

12.2.1.1 ASE noise/OSNR

Optical amplification, most commonly realized using EDFAs, is accompanied by ASE noise. The variance of signal-spontaneous beat noise can be observed in the electrical waveform of the signal as a fluctuation around the signal level value. In OOK systems, the noise level can be related to a performance parameter called the Q-factor, which can be used to estimate system BER. However, in phase-modulated systems, the output of the balanced receiver is based on the phase component and noise distribution is non-Gaussian. Therefore, the Q-parameter cannot be used as a reliable method to determine the BER in phase-modulated systems.[25]

The performance of a beat noise–limited receiver can be fully characterized by the level of optical signal-to-noise ratio (OSNR) necessary to obtain a target BER.[19] For this reason, a reduction in OSNR reduces the margin for other system impairments. The OSNR is customarily defined independently of the data rate in an optical resolution bandwidth B_o of 0.1 nm. The reported OSNR required to achieve BER of $1 \cdot 10^{-9}$ in an RZ-DQPSK signal at 20 Gb/s is approximately 17.5 dB.[26] The RZ-DPSK signal at the same bit rate requires 2.3 dB less OSNR to achieve the same BER.[27] It has to be stressed that the required OSNR measured in a fixed-resolution bandwidth is increased by 3 dB for every doubling in signal bit rate.

12.2.1.2 Chromatic dispersion

While the level of ASE-related OSNR reduction scales with the number of traversed amplifiers, the influence of CD scales with the length of transmission fiber. Moreover, it scales with the square of the bit rate, as the spectrum of a higher bit rate signal is wider and the bit period is shorter. The uncompensated CD results in receiver penalty. In the case of phase-modulated signals, a 2-dB penalty occurs for accumulated CD of 32 ps/nm in a 42.7-Gb/s RZ-DPSK signal[28]; this

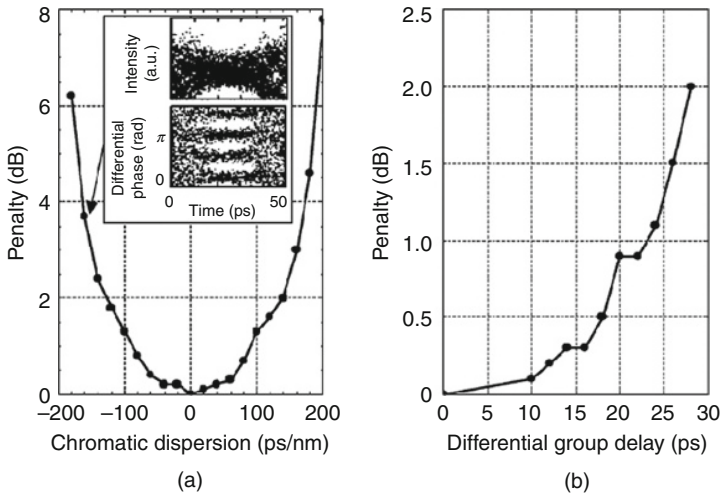

FIGURE 12.2

(a) Power penalty as function of accumulated chromatic dispersion for 42.7-Gb/s RZ-DQPSK signal. (b) Power penalty as function of DGD for 42.7-Gb/s RZ-DQPSK signal.[27]

corresponds to 512 ps/nm in a 10-Gb/s signal. In the case of an RZ-DQPSK signal, the same penalty of 2 dB was reported for accumulated CD of 130 ps/nm in a 42.7-Gb/s signal, as seen in Figure 12.2(a). This corresponds to 520 ps/nm in a 20-Gb/s RZ-DQPSK signal.[27] The agreement between these results stems from the fact that the 10-Gb/s RZ-DPSK and 20-Gb/s RZ-DQPSK signals occupy the same bandwidth and have the same symbol rate.

12.2.1.3 Polarization mode dispersion

Apart from CD, PMD is another dispersive process affecting the quality of optical transmission. It occurs as a result of random deviations from the circularity of the fiber causing birefringence between the polarization axes.[29]

The optical signal, ideally consisting of two degenerate modes, experiences a polarization-dependent differential group delay (DGD) during transmission. Random coupling between the states of polarization due to fiber stress or nonlinear birefringence lead to fluctuations of DGD in time. This makes PMD more difficult to control and compensate than CD.[30] Unlike in the case of CD, where the amount of temporal spreading is related to the optical bandwidth of the signal, the (first-order) PMD is independent of the frequency of signal components.

The penalty induced by PMD on the optical channel depends predominantly on the waveform of the signal. For that reason, the influence scales linearly with signal bit rate.[19] The DPSK signals generally perform better than the OOK signals,[9] and in the case of a 42.7-Gb/s DPSK, a penalty of 2 dB was reported at a PMD-induced DGD of 14 ps.[28] The RZ-DQPSK signal has been shown to perform significantly better than both DPSK and OOK due to the reduced symbol rate for a given bit rate.[19,31] The 42.7-Gb/s RZ-DQPSK signal suffers a 2-dB penalty at DGD of 28 ps, as seen in Figure 12.2(b). In both cases, the 2-dB penalty occurs at a DGD of approximately 50% of symbol duration.

12.2.1.4 Filtering and frequency offset

An important penalty source in optical networks stems from signal spectrum filtering in reconfigurable optical add-drop multiplexer (ROADM) filters of multiple optical nodes. The impact of spectrum narrowing on the performance of DPSK signals has been studied in Reference 24. It has been shown that the DPSK modulation with balanced detection increases the robustness to optical filtering due to the better tolerance to intersymbol interference (ISI), as seen in Figure 12.3(a). In the case of DQPSK modulation, the reduced spectrum of the signal ensures that the penalty due to filtering is significantly lower than in the case of DPSK of the same bit rate.[19] For a 40-Gb/s signal it reaches 1 dB after transmission over 10 filter stages with a bandwidth of 44 GHz.[27] This has also been confirmed for PolMux DQPSK signals.[32]

The stated values of a filtering penalty are obtained under the assumption that the frequency of the optical carrier matches the predetermined grid and is aligned with all-optical components in the signal path. Without the proper supervision, the center frequencies of optical components will vary with time and fluctuate due to environmental factors. The frequency drift of the lasers or the optical components leads to relative frequency misalignment in the network and may cause optical power loss, crosstalk between channels, or penalty in the delay interferometer used for the demodulation of a DPSK or DQPSK channel. For a 40-Gb/s DPSK signal, a 1.2-GHz frequency offset in the demodulator leads to a power penalty of 1 dB.[33] For the same bit rate, a 1-dB penalty in the DQPSK is incurred at only a 0.2-GHz frequency offset. Both cases are illustrated in Figure 12.3(b).

Finally, it should be noted that the laser linewidth also has an influence on the performance of phase-modulated channels. In the case of DQPSK signals, the laser phase noise stemming from the nonzero

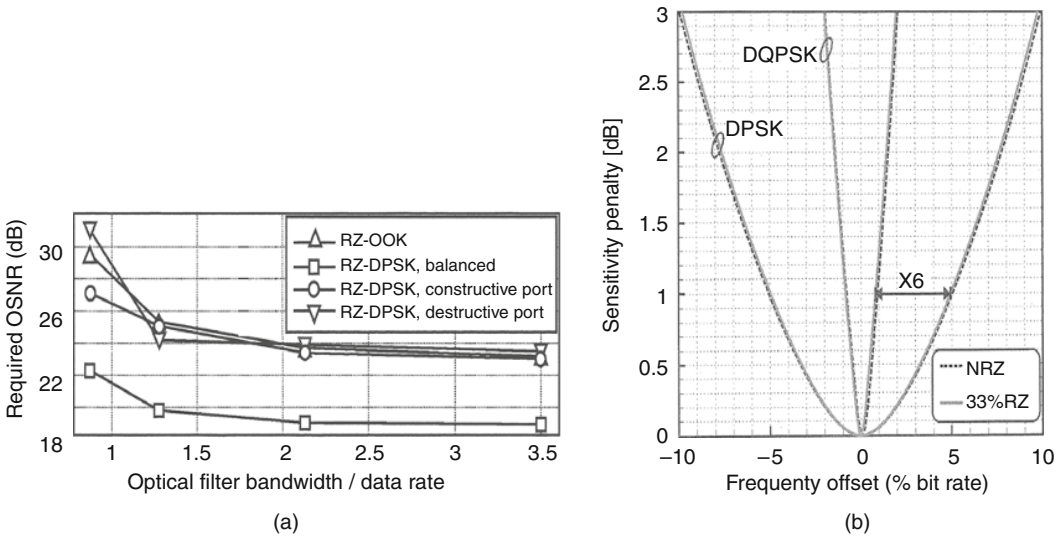

FIGURE 12.3

(a) Comparison of robustness to optical filtering for OOK and RZ-DPSK formats.[24] (b) Sensitivity penalty as function of frequency offset for DPSK and DQPSK format.[33]

linewidth of the laser was shown to impair the tolerance to accumulated CD.[34] The influence of laser linewidth is even more pronounced when the number of phase levels is increased.[35]

12.2.1.5 Nonlinear phenomena

Linear impairments described in the preceding sections affect the performance of optical signals in proportion with the traversed distance, number of optical amplifiers, and signal bit rate. Another group of transmission effects influencing the quality of the signal is dependent on optical power. The origin of nonlinear phenomena stems from the confinement of transmitted light to the small effective area of the fiber core, which results in high optical densities influencing the refractive index of silica through the optical Kerr effect. As the intensity of the optical field changes due to modulation of the signal amplitude, signal-induced refractive index fluctuations affect the phase of the optical signal. During transmission in dispersive fiber, the fluctuations in phase are converted into intensity variations, which distort the waveform shape.[3]

The influence of nonlinear phenomena on the signal depends on the employed modulation format as well as characteristics of the optical transmission platform. For systems with low SE, phenomena such as four-wave mixing (FWM), XPM, and self-phase modulation (SPM) have to be taken into account. When a low-dispersion fiber, such as a non-zero dispersion-shifted fiber (NZ-DSF), is employed, the FWM is the dominant effect.[3] The phase-modulated formats are affected by the nonlinear phenomena to a lesser degree.[36] The higher receiver sensitivity of the RZ-DPSK as well as the RZ-DQPSK format allows transmitting the signal with lower power compared to the OOK case, while achieving the same BER.[7] This allows reducing the effect of nonlinear phenomena. Moreover, the RZ pulse carving was shown to reduce the distortion due to XPM for the RZ-DPSK[11] and RZ-DQPSK signals.[37] Because the waveform pattern is not dependent on data and does not change from bit to bit, the effect of XPM averages as the neighboring WDM channels pass each other due to CD. Therefore, no timing jitter is introduced to the signal.[6] At symbol rates of 40 Gb/s and channel spacing of 100 GHz, both RZ-DPSK and RZ-DQPSK improve resilience to nonlinear phenomena by 3 dB, compared to OOK signals.[27,37]

Despite improved tolerance to XPM, the phase-modulated transmission is susceptible to another form of impairment stemming from nonlinear signal-noise interactions. The nonlinear phase noise (NPN), also called Gordon-Mollenauer noise, results from the conversion of amplitude fluctuations into phase fluctuations.[38] The influence of NPN is especially pronounced in long-haul transmission systems[39] and in the case where OSNR is poor during the transmission (regardless of the receiver OSNR).[19] The most important types of signal-noise interactions are the SPM-induced NPN and the XPM-induced NPN.[40] The random intrachannel (SPM) or interchannel (XPM) amplitude fluctuations are translated into phase modulation, which results in a penalty in the DPSK and DQPSK signal during reception. The penalty is stochastic and depends on the signal power and propagation distance, as well as the level of noise in the signal.[34,41] Low-CD fibers increase the effect of NPN, as is also the case for other nonlinearities. The effect is most pronounced for signals in low symbol-rate systems where long coherence time is required. Moreover, the phase-modulated channels with differential receivers (DPSK) show higher sensitivity to NPN than the formats not employing self-homodyne reception (PSK).[42,43] It has been reported that phase noise cancels the 3-dB sensitivity advantage of the differential receiver.[41] In the case of multilevel modulation formats, the penalty due to the NPN is expected to be larger than that of DPSK due to smaller spacing between the points in the constellation diagram.

12.2.2 Generation and detection of N-PSK signals

The advantageous properties of phase-modulated formats come at a price of complexity in transmitter and receiver structures, compared to the OOK transmission. DPSK modulation can be performed either by a phase modulator (PM) or by a Mach-Zehnder modulator (MZM) biased at zero transmission and driven at twice the switching voltage.[8] If a phase modulator is used, a constant-envelope signal is generated; however, the phase transitions between bits are not instantaneous and introduce chirp. Employing the MZM allows switching the phase between consecutive symbols precisely by π. The latter approach introduces residual amplitude modulation and is illustrated in Figure 12.4(a). The two neighboring transmission maximum points have opposite phase, which produces a phase shift of π regardless of drive voltage imperfections. Conversely, in the case of PM, the optical phase directly follows the electrical signal. Therefore, the phase transitions are limited by driver bandwidth and the imperfections of drive signal are reflected in phase distortions. The chirp or fluctuations in intensity can be suppressed in RZ-DPSK format, in which case an additional pulse carver is employed.

DQPSK signal generation requires a more complicated modulator structure, imprinting the in-phase and quadrature data components. The modulators can be arranged either in parallel or serial fashion. Respective arrangements are presented in Figures 12.4(b) and (c). In the parallel arrangement, continuous-wave (CW) light is split between two nested MZMs operating as phase modulators. The phase of the optical carrier is modulated at the symbol rate producing dual DPSK signals. The phase of one of the DPSK tributaries is rotated by $\pi/2$, and subsequently the signals are combined. The

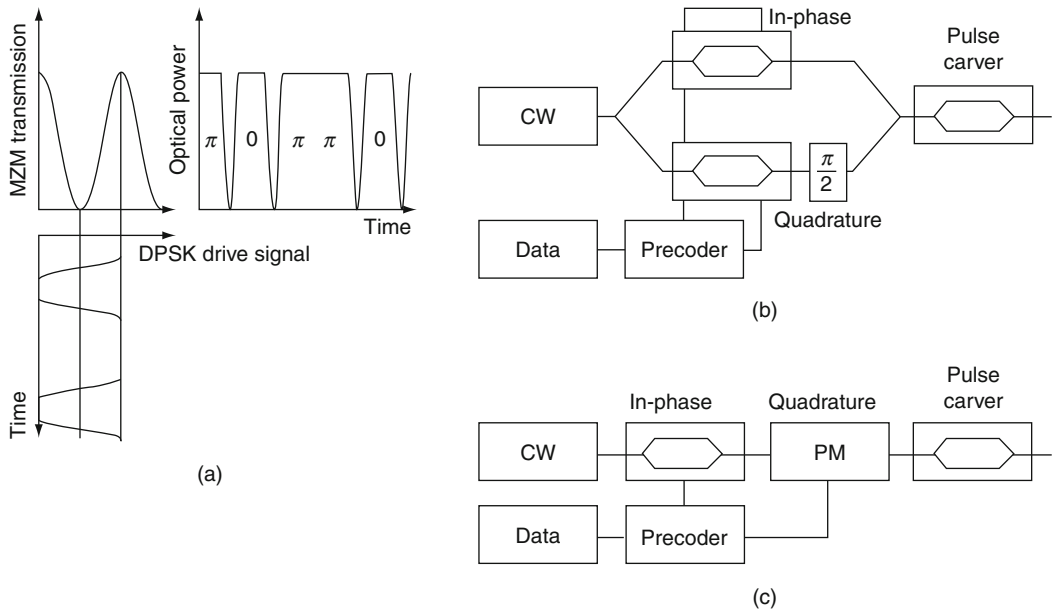

FIGURE 12.4

Phase modulation of the optical signal: (a) generation of DPSK signal using MZM, (b) generation of RZ-DQPSK in parallel configuration, and (c) generation of RZ-DQPSK in serial configuration.

resulting field is a DQPSK signal with the bit rate equal to the sum of symbol rates in the tributaries. A pulse carver adds the RZ shaping to create the RZ-DQPSK signal. This arrangement provides modulator stability and precise carrier-phase modulation.[3] The serial arrangement, presented in Figure 12.4(c), uses an MZM to generate the 0 or π in-phase component and a phase modulator to add the $\pi/2$ quadrature component. As in the previous case, a pulse carver is necessary to generate the RZ-DQPSK signal. The latter modulation scheme can be realized using discrete components.[44] Other modulator structures have also been proposed in the literature. Details can be found in Reference 45 for generation of RZ/CSRZ-DPSK signals and in Reference 46 for DQPSK signals. The generation of a higher number of signal levels has been shown using the adaptation of the described modulators.[47]

The noncoherent phase-modulated systems use direct detection at the receiver. However, the square-law detection of a photodiode (PD) is not sensitive to the phase of the optical carrier. For that reason, a delay interferometer (DI) is inserted in the path of the signal in order to convert the phase modulation into amplitude modulation. Typically, a Mach-Zehnder interferometer (MZI) is employed. An MZI followed by a balanced receiver is shown in Figure 12.5(a).

The multilevel phase encoding in the DQPSK signal requires a more complicated receiver structure. Typically, it consists of a pair of MZIs, as shown in Figure 12.5(b). The delay introduced by the interferometers is equivalent to the symbol rate. Contrary to the case of DPSK, in DQPSK, the MZIs introduce a differential optical phase shift between the branches. The differential phase is equal to $\pi/4$ and $-\pi/4$ for the upper and lower branch, respectively. The output voltage signals after balanced detection are proportional to $\cos(\Delta\varphi i) + \sin(\Delta\varphi i)$ and $\cos(\Delta\varphi i) - \sin(\Delta\varphi i)$, where $\Delta\varphi i$ is the differential phase shift between the neighboring symbols. This produces the in-phase (I) and quadrature (Q) data components, respectively.[48] The complex structure of the DQPSK receiver causes an approximate 1-dB power penalty.

Proper operation of the optical receiver has a major impact on the performance of both DPSK and DQPSK signals.[8] For balanced DPSK detection, the detector amplitude imbalance of 40% will result in a 1-dB OSNR penalty. Similarly, a 1-dB OSNR penalty may be expected when the delay imbalance between the detector arms reaches 0.4 of the symbol period. Finally, a receiver detuning by frequency equal to 2% of signal bit rate will cause an OSNR penalty of 1 dB. In the case of DQPSK signals, the amplitude imbalance causing an OSNR penalty of 1 dB is also approximately 40%.[49] The penalty due to delay imbalance varies depending on signal shaping. In the case of RZ-DQPSK modulation, the OSNR penalty reaches 1 dB at a delay imbalance of 0.4 of the symbol period.[50] The sensitivity to frequency detuning is increased and results in an OSNR penalty of 1 dB for a detuning of 1.7% of the symbol rate.

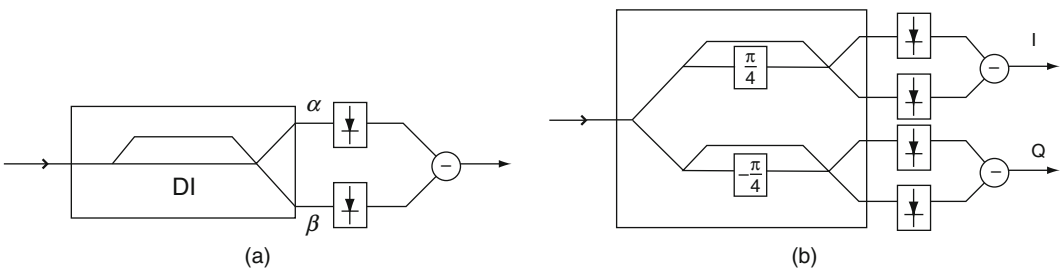

FIGURE 12.5

Demodulator and balanced receiver for (a) DPSK and (b) DQPSK.

12.3 OPTICAL PERFORMANCE MONITORING

Optical performance monitoring (OPM) techniques provide the means to analyze signal quality directly in the optical domain. The quality is estimated in terms of a single performance parameter. Currently, monitoring performance in the physical domain involves individual component alarms or optical power, inferring that the performance is satisfactory if optical components operate within the assumed limits and the optical channels are present.[51] However, the target for OPM is the development of more sophisticated parameters, allowing the analysis of signal quality. Apart from signal power and OSNR, which are the most commonly considered impairments,[52,53] accumulated CD and PMD are the parameters that can provide insight into optical channel performance.[54] When considering phase-modulated transmission systems, additional factors need to be taken into consideration. The first is the laser frequency offset, which incurs a power penalty at the receiver. The second is the phase noise, which may stem from the nonzero laser linewidth or from nonlinear conversion of ASE into phase fluctuations.

In the following sections, the techniques for monitoring the dominant impairments affecting the DPSK and DQPSK signals are described. First, the methods for estimating and suppression of NPN are presented in Section 12.3.1.1. Although these techniques do not provide feedback upon which signal quality can be estimated, they have been shown effective in reducing the penalty by monitoring optical waveform parameters. Next, the group of techniques monitoring the optical spectrum for estimation of the OSNR is discussed in Section 12.3.1.2. These techniques are shared with other modulation formats, and this section only discusses the merits and demerits of existing approaches. Subsequently, Section 12.3.1.3 focuses on monitoring techniques based on polarization nulling and DOP monitoring. Section 12.3.1.4 explains the group of techniques based on measurements of electrical radio frequency (RF) spectrum and clock tone. In Section 12.3.1.5, the techniques exploiting pilot tones are presented. While Sections 12.3.1.2 through 12.3.1.5 discuss the monitoring techniques observing the signal spectrum, the methods presented in Sections 12.3.1.6 through 12.3.1.8 focus on methods analyzing waveform samples. Section 12.3.1.6 discusses the application of linear optical sampling and phasor-based monitoring to phase-modulated signals. Sections 12.3.1.7 and 12.3.1.8 explain the methods of asynchronous sample analysis with histograms and two-tap plots, respectively. Finally, in Section 12.3.1.9, other monitoring techniques employing a receiver and signal processing are presented. Section 12.3.2 summarizes and compares the presented OPM techniques.

12.3.1 Monitoring techniques

12.3.1.1 Nonlinear phase noise compensation

As mentioned in Section 12.2.1.5, the NPN stems from the interaction of ASE noise generated in the amplifiers and the signal through the fiber's nonlinear refractive index. As a result, the fluctuations in intensity change signal propagation speed, influencing the signal phase. The relationship between the intensity fluctuation and phase noise has been employed as a feedback mechanism to counteract the adverse effects of NPN. Although there have been no reports on developing the parameter for quantifying the level of NPN for monitoring purposes, several techniques suppressing phase noise using the feedback signal have been presented in the literature.

In one approach, a phase noise compensator consisting of a power monitor and phase modulator was proposed.[55,56] A broadband photodetector placed before the receiver analyzes the incoming signal power to determine the amount of phase rotation necessary to counter that incurred through

the Kerr effect. The phase rotation is subsequently applied in the phase modulator. The proper adjustment of the amount of phase rotation and delay enables increasing the OSNR margin by 2.5 dB under the nonlinear transmission regime. This scheme has been shown to further improve DPSK signal performance in the nonlinear regime for a multispan transmission when polarization diversity is added to the compensation scheme.[57]

The principle of opposite-phase rotation correlated to instantaneous power fluctuation has also been demonstrated using nonlinear elements. In Reference 58, the periodically poled $LiNbO_3$ waveguide provides a negative nonlinear phase shift, reducing the Q-penalty by approximately 6 dB for a single channel. The efficiency of this technique is reduced for a DWDM system due XPM-NPN, in which case a Q-penalty reduction of approximately 3 dB is observed.

A different approach to compensating the NPN using nonlinear elements was shown in Reference 59. The DQPSK transmission is precompensated by a phase-preserving amplitude limiter. Employing FWM saturation in a highly nonlinear fiber (HNLF), the fluctuation of amplitude of the pulses is suppressed at the transmitter. This allows increasing the transmission power in a densely dispersion-managed system by 5 dB without incurring the penalty due to NPN.

The compensation of nonlinear phase rotation was also demonstrated using numerical methods after signal reception. In Reference 60, the boundary decision threshold of the receiver was modified to follow the after-transmission spiral rotation of the phase, as shown in Figure 12.6(a). The constellation of a DPSK signal is restored by using a lookup table or phase subtraction correlated to the signal power, thereby reducing the standard deviation of NPN and suppressing the nonlinear phase rotation (Figure 12.6(b)). A similar phase-compensation approach in a digital coherent receiver is presented in Reference 61.

The level of NPN affecting performance of the phase-modulated channels is dependent not only on the power and distance of transmission but also on the level of launched OSNR. The following section briefly discusses demonstrated techniques for spectral monitoring of OSNR in optical links.

12.3.1.2 OSNR/power monitoring

The monitoring of optical power and OSNR through optical spectrum analysis is the most basic OPM method and the only one that has been standardized.[62] It is also largely modulation-format independent. It compares the optical power contained in the signal to the power of ASE, typically within a bandwidth of 0.1 nm. It has been shown that the monitor placed within an optical network needs to provide information about the level of OSNR for levels of up to 26 dB for a 10-Gb/s signal.[53] However, the analysis of spectrum of a DWDM signal transmitted over OADMs is likely to provide incorrect measurements as the densely spaced channels will obscure the level of OSNR. Moreover, channels with different OSNR levels are added and dropped and the ASE is shaped by the optical filters.[63]

A spectrum-based, OSNR monitoring technique solving the above issue has been presented for OOK and DPSK signals.[64] It is based on cascaded, long-period fiber gratings equipped with an optically tunable phase shifter. The first grating splits the signal into a core mode and cladding mode that are recombined in the second grating. The optically tunable phase shifter, consisting of an Ytterbium-doped optical fiber, controls the phase difference between the core and cladding modes. Depending on the relative phase between the modes, either the power of incoherent ASE noise or the combined power of coherent signal and ASE noise can be measured, allowing the calculation

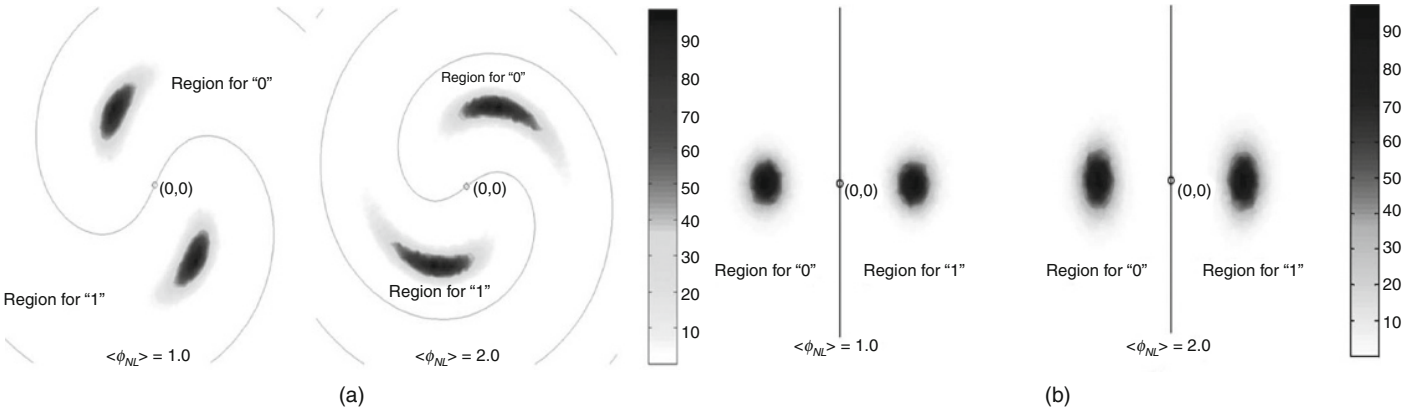

FIGURE 12.6

(a) Phase distribution and decision regions of received signals with NPN for nonlinear phase shift of 1 rad (left) and 2 rad (right). (b) Corrected signal distribution for nonlinear phase shift of 1 rad (left) and 2 rad (right).[60]

of OSNR within the channel. The method was shown to provide an OSNR monitoring range from 0 to 28 dB without being influenced by the accumulated CD or PMD. A similar interferometer-based, OSNR monitoring technique using a partial-bit-delay interferometer was demonstrated for a 40-Gb/s DPSK signal.[65] The monitoring range of 5–25 dB was shown to be independent of the influence of both CD and PMD.

12.3.1.3 Polarization nulling and DOP monitoring

The OSNR monitoring based on polarization nulling is an alternative to the spectrum-based OSNR monitoring and has been first presented in Reference 66. Basing on the assumption that the signal is contained in a single polarization, while the ASE noise is uniformly distributed between the polarizations, the monitoring of OSNR using a slowly rotating quarter-wave plate and a linear polarizer was demonstrated. By measuring the maximum and minimum optical power passing these two elements, the ratio between the signal and noise power can be extracted. The method was further refined through additional parameters and signal filtering in order to address the problem of signal depolarization due to PMD, or partial polarization of ASE due to polarization-dependent loss (PDL).[67] Polarization nulling has been shown effective in monitoring the OSNR of RZ-DPSK signals from 22 to 33 dB.[68]

A different approach toward monitoring impairments using signal polarization is based on analysis of the degree of polarization (DOP). It has been demonstrated both without[69] and with[70] polarization scrambling at the transmitter. The OSNR can be measured as a function of signal depolarization due to the presence of unpolarized ASE noise. Apart from OSNR monitoring, the DOP-based technique has been shown effective in monitoring the influence of PMD in phase-modulated signals.[71] PMD causes temporal misalignment between signal components traveling in the orthogonal states of polarization. The difference in arrival time between the two polarizations at the receiver reduces the signal's DOP. For a DPSK signal, the DOP has been shown to provide unambiguous measurement of PMD for DGD values of up to 1.0 symbol period for the NRZ-DPSK format and 0.5 symbol period for RZ-DPSK. Similar results have been presented for the DQPSK modulation.[72]

12.3.1.4 RF spectrum/tone monitoring

In contrast to the OPM techniques presented in Section 12.3.1.2, which utilized the optical spectrum, this section focuses on the electrical RF spectrum of the received optical channel. The RF spectrum corresponds to the power spectrum of the intensity, and is affected by optical impairments such as reduction in OSNR, CD, or PMD. This makes analysis of the RF spectrum a powerful tool for OPM.

In the case of OOK modulation, the RF spectrum contains a strong component stemming from data modulation. In comparison, the RF component originating from signal beating and ASE noise in the receiver is relatively small. This makes the RF spectrum–based monitoring of OSNR in intensity-modulated systems impractical. However, in the case of phase-modulated signals, the power spectrum does not bear the data information, and is therefore lower than in OOK systems. The low-frequency components of the phase-modulated signal do not change even in the presence of accumulated CD. The small background (signal) RF component allows monitoring the power of the beat component between the ASE noise and the signal at low frequencies. This property has been employed in evaluating the level of OSNR.[73] A slow optical detector with an electrical bandpass filter (BPF) is used to monitor the OSNR from 15 to 35 dB by observing the power around the 6-MHz frequency.

Similarly, a low-frequency RF component was used to monitor the OSNR level in a single-channel 80-Gb/s PolMux RZ-DPSK signal.[74] A narrowband optical filter is used to extract a portion of the optical signal spectrum and ASE noise after an EDFA. Assuming a constant power level after

the filter, the ratio of signal power to the power of noise is reduced with the OSNR reduction. Observation of the RF spectrum component in the vicinity of 250 MHz enables OSNR monitoring from 11 to 29 dB. The use of low-frequency components ensures that the method is not influenced by accumulated CD or PMD.

A modification of this technique also allows tracking of the PMD level. Observation of low-frequency components in an 80-Gb/s PolMux RZ-DPSK signal was shown effective in PMD monitoring from 0 to 12 ps.[75] This method takes advantage of the interaction between two signals in orthogonal polarizations after the polarizer and is illustrated in Figure 12.7. The polarizer is aligned with the polarization of one of the data streams. When no PMD is affecting the signal, there are no observable intensity components in the RF spectrum. However, in the presence of PMD, the orthogonal signals become depolarized and the crosstalk component between them can be observed after the polarizer. The observation of frequency tone in the vicinity of 250 MHz provides a CD-independent evaluation of PMD. It must, however, be noted that the sensitivity of the monitor depends on alignment precision between the polarizer and the polarization-multiplexed channel.

Higher-frequency components of the DPSK signal are more susceptible to CD influence. The phase components of the signal are converted to intensity fluctuation with the accumulation of CD, which makes them appear in the RF spectrum of the signal. In contrast to OSNR monitoring with a low-frequency BPF, a high-frequency BPF can be used to observe the level of phase-to-amplitude conversion, and therefore to monitor the level of accumulated CD. This approach was assumed in Reference 76, where a broadband BPF is used to observe the CD. The monitoring range is dependent on filter bandwidth, and for a 10-GHz-wide filter, at which the method showed the

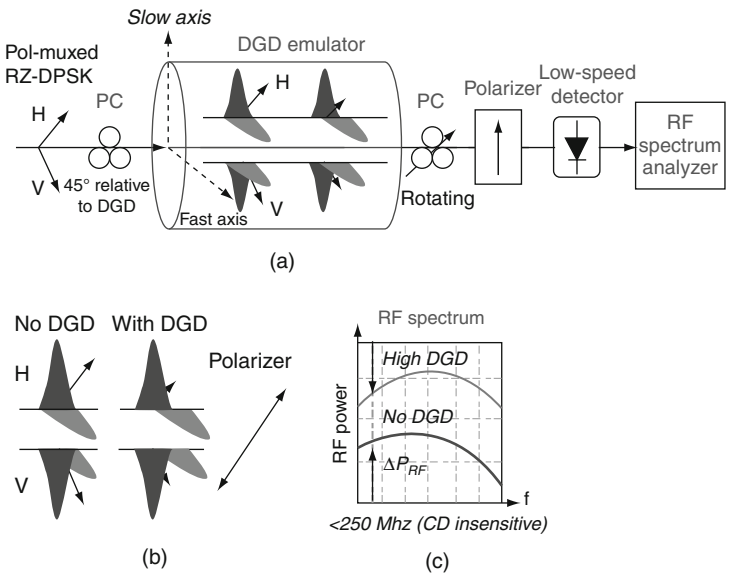

FIGURE 12.7

(a) Diagram of CD-independent PMD monitoring technique. (b) Alignment of polarizer with respect to signal in case without and with DGD. (c) Variation of RF spectrum power depending on level of DGD.[75]

highest sensitivity, the monitoring range reached from 0 to 800 ps/nm. The method was shown to limit the influence of OSNR on the monitoring result by analyzing the RF power within two independent frequency bands.

The phase-to-amplitude conversion of the RZ-DPSK signal was also used for monitoring the level of accumulated CD in conjunction with CW probe and fiber nonlinearity.[77] The CD-induced fluctuation of intensity in the phase-modulated signal is transferred to the probe through XPM in a highly nonlinear fiber. By measuring the degree to which the XPM modulates the CW light, the level of accumulated CD can be estimated up to 120 ps/nm for a 40-Gb/s RZ-DPSK signal. This method can also potentially be used for an 80-Gb/s RZ-DQPSK signal with a similar monitoring sensitivity.

A particular case of RF spectrum monitoring is observation of the clock tone level. Accumulated CD causes a relative delay between the upper and lower sidebands of the signal. In the case of RZ-shaped, phase-modulated channels, the clock component in the RF spectrum will fade and rise periodically with the increase in CD due to the interference of components in the two sidebands. For the NRZ-shaped signals, these clock components are out of phase when the CD equals zero and produce no clock component in the RF spectrum. As the amount of accumulated CD is increased, the clock components interfere constructively. This phenomenon has been used to estimate the level of accumulated CD in NRZ-DPSK and RZ-DPSK signals.[71] For 10-Gb/s signals, the measurement ranges from 0 to 600 ps/nm and 0 to 900 ps/nm for NRZ-DPSK and RZ-DPSK, respectively. In a system employing 10-Gb/s DQPSK modulation, the clock tone measurement showed sensitivity to the level of accumulated CD up to 720 ps/nm.[72]

In the abovementioned technique, the clock level is related to the amount of accumulated CD. However, the clock tone level is also influenced by PMD, resulting in ambiguity and possible measurement errors. A technique that allows monitoring of both CD and PMD in OOK and NRZ-DPSK signals was presented in Reference 78. It analyzes the RF clock power at the output of an unbalanced DI. The principle is illustrated in Figure 12.8. The DI has a quarter-bit delay in one arm. Inside the DI, the original signal interferes with itself for 75% of the bit period and with the phase of the following bit for 25% of the bit period. At the output, the constructive port introduces almost no change to the signal due to the large free spectral range (FSR) of the interferometer. The destructive port filters signal sidebands, leading to an RZ pulse train at its output. The 10-GHz clock at the output of both arms of DI is used to independently analyze CD and PMD. The clock power from the constructive port grows with an increase in CD and a decrease in PMD. Conversely, the clock from the destructive port grows with the decrease in both CD and PMD. Using these observations, CD can be evaluated from 0 to 600 ps/nm and PMD from 0 to 50 ps for a 10-Gb/s NRZ-DPSK signal.

12.3.1.5 Pilot tone monitoring

The monitoring techniques described in the previous sections are based on the inherent properties of the signal's optical or electrical spectrum. Optical impairments that affect signal quality also influence certain features of the spectrum. This concept is extended by introducing a distinct frequency tone that can be observed regardless of the information-carrying portion of the signal. The tone format, frequency, and intensity are designed to reflect the optical impairments affecting the signal during transmission. This principle is employed in OPM techniques based on pilot tones.[79]

The pilot tone monitoring techniques require a modification to the transmitter, which is illustrated in Figure 12.9. A low-frequency RF-modulated tone is added to the optical channel. The tone may modulate the amplitude, frequency, or phase of the carrier. It may be added through

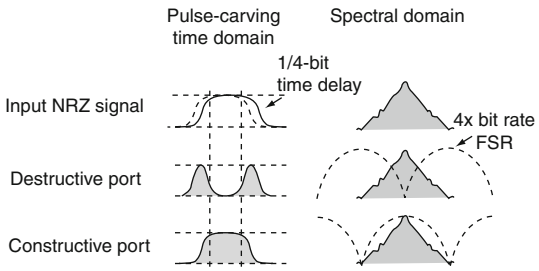

FIGURE 12.8

Partial-bit DI for NRZ signal monitoring. Fraction of bit interferes with following bit, which leads to pulse carving in destructive port. Pulses produce a strong clock tone.[78]

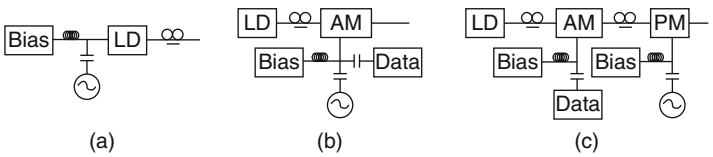

FIGURE 12.9

Modification to transmitter for pilot tone monitoring techniques.[79]

modulation of the laser diode bias (Figure 12.9(a)) or through an external-intensity or phase modulator (Figures 12.9(b) and (c)).[80] At the receiver, the tone can be filtered from the signal using a BPF after the PD and analyzed using an RF power detector. The drawbacks of this method are the necessity to modify the transmitter and the degradation in receiver sensitivity of the monitored signal due to reduced extinction ratio, crossgain modulation in optical amplifiers, or stimulated Raman scattering.[79]

The realization of an intensity-modulated, pilot tone monitoring technique in phase-modulated systems has been shown to have a relatively small impact on the signal. Since the intensity spectrum of the phase-modulated channels does not contain low-frequency components, the power of pilot tone can be reduced while maintaining the tone-to-signal ratio, as shown in Figure 12.10. Using this method, a 300-MHz tone was employed to monitor the optical signal power, wavelength, and path in the optical DPSK signal.[81] However, when compared to the pilot tone monitoring of the intensity-modulated channels, monitoring of transmission impairments has not been realized due to the tone's low frequency.

The pilot tone monitoring technique is not limited to intensity-modulated tones. The phase-modulated pilot tone has been shown effective in monitoring the frequency offset between the signal and the demodulator DI.[82] A low-modulation index-phase dither tone is added to the DPSK signal. At the receiver, the dithered phase is converted to intensity in the DI when the center frequency of the channel and the interferometer does not match. The power of the recovered tone is proportional to the frequency offset and allows monitoring the detuning of the demodulator from -2 to 2 GHz with a resolution of 1 MHz. Similarly, in Reference 83 an intensity tone with a frequency equal

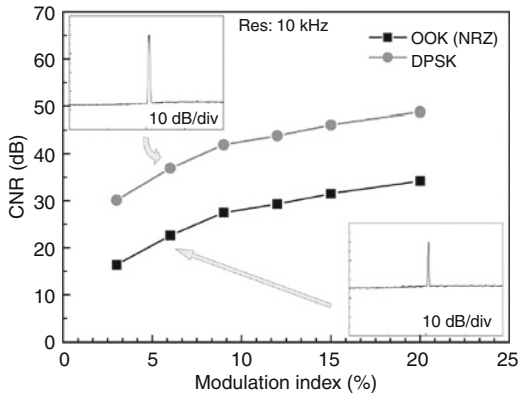

FIGURE 12.10

Improvement of carrier-to-noise ratio (CNR) in DPSK signal over OOK signal for pilot tone monitoring technique.[81]

to half of the signal bit rate was used to monitor the frequency offset between the optical source and the demodulator. In this case, however, the presence of tone resulted in a power penalty of 0.4 dB.

12.3.1.6 Linear optical sampling and phasor monitoring

The OPM techniques described thus far in this chapter have been focused on analyzing the properties of optical or electrical signal spectra that are influenced by transmission impairments. These techniques are popular because, in most cases, they do not require high-speed components. However, transmission impairments primarily influence the signal waveform. Accordingly, a number of monitoring techniques have been developed for direct signal analysis. Traditionally, the waveforms are characterized by measures such as rise and fall time, extinction ratio, or jitter. These values are calculated from the intensity eye diagrams of the sampled optical waveform.[84] The introduction of phase–modulation formats opened a new field for sampling-based OPM. On the one hand, a new set of parameters had to be developed for analyzing intensity samples, as the waveforms are different from OOK systems. On the other hand, sampling techniques enabling the analysis of signal constellation provided new insight into both intensity and phase evolution of the channel. This section describes the OPM techniques that analyze the optical field based on samples acquired using linear optical sampling and self-homodyne phasor monitoring.

Linear optical sampling is a technique for capturing optical signal intensity and phase with high temporal resolution. The signal is mixed with optical pulses generated by a local source. A 90° optical hybrid splits and recombines the two fields while introducing 0 and $\pi/2$ relative phase shifts. The interference patterns are received by balanced photodiodes, as shown in Figure 12.11. Interference between the two fields is used to recover the incoming signal's intensity and phase. The use of short, repetitive optical pulses for the local oscillator forms a gate for the sampling process, thereby reducing the requirement for high-speed electronic sampling components.[85]

Linear optical sampling allows analysis of signal constellations generated by optical phase–modulated sources. It is capable of revealing modulation distortion and OSNR degradation, as

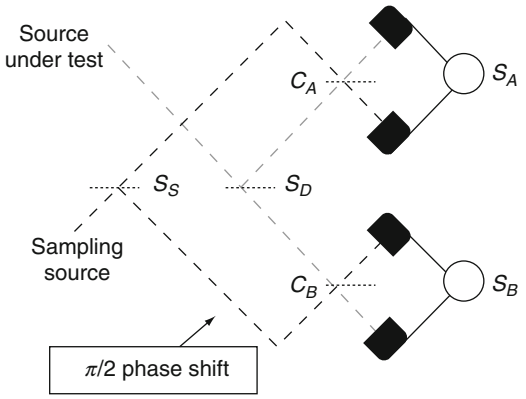

FIGURE 12.11

Diagram of optical circuit for mixing of optical signal with local oscillator light (90° optical hybrid).[81]

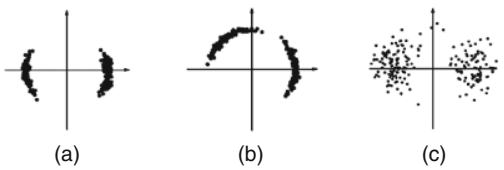

FIGURE 12.12

Signal constellation obtained using linear optical sampling: (a) PSK signal modulated with MZM, (b) signal modulated with PM at driving voltage of $2/3V_{\Pi}$, and (c) PSK signal with OSNR = 13 dB.[85]

illustrated in Figure 12.12. Figure 12.12(a) presents a constellation diagram of a PSK signal modulated by MZM. The phase noise is relatively small, while the noise stemming from imperfections in the drive signal introduces a minor variation in samples along the real axis. Alternatively, a constellation diagram of a PSK signal generated by a phase modulator driven by voltage of $2/3V_{\Pi}$ is shown in Figure 12.12(b). The incomplete inversion of phase and the phase noise stemming from the drive signal noise can be clearly observed in the constellation diagram. Finally, Figure 12.12(c) shows the effect of ASE noise on the constellation diagram when the OSNR of the signal is reduced to 13 dB.

Analysis of the obtained constellation diagrams allows quantifying the amount of signal distortion.[86] Taking Figure 12.12(c) as an example, by calculating the variance of samples in phase or amplitude around the mean value of the symbol, it is possible to estimate the level of ASE noise. This value is directly related to OSNR when normalized to the signal's average power. An example of OSNR measurement using this technique is shown in Figure 12.13(a). Moreover, the correlation between the intensity and phase of the sample in the constellation diagram can be used for estimation of the NPN affecting the phase-modulated signal. The correlation has been used as the parameter in estimating the NPN level, showing a linear relationship to the signal power before transmission, as demonstrated in Figure 12.13(b). The linear optical sampling technique also allows monitoring of

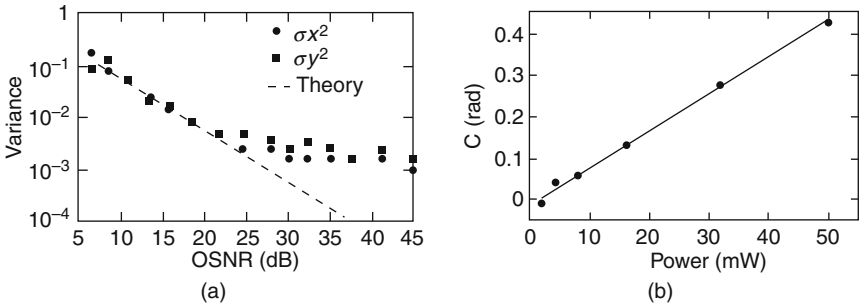

FIGURE 12.13

(a) Evaluation of OSNR using linear optical sampling. (b) Evaluation of NPN using linear optical sampling.[86]

multilevel phase-modulated signals, as was demonstrated in Reference 87 for a 43-Gb/s RZ-QPSK signal. Similar to the case of PSK signal monitoring, the statistical distribution of samples allows monitoring the OSNR level, while the correlation between the phase and amplitude values provides a parameter for evaluating the level of NPN.

The ability to measure the performance of phase-modulated channels provided by the constellation diagrams has attracted research toward the development of techniques allowing simple acquisition of both intensity and phase information of the signal. One such example is the self-homodyne phasor monitor presented in Reference 88. The monitor consists of a delay interferometer and a 120° optical hybrid followed by three optical detectors, as shown in Figure 12.14(a). The output of the detectors is sampled and based on the three values, and the phase and intensity of the samples are calculated in the constellation diagram, as shown in Figure 12.14(b). The relative phase between the arms of the delay interferometer is not matched exactly to the operating wavelength; therefore, the obtained constellation is rotated by an angle δ. The rotation is compensated numerically by calculating the differential phasor indicating the real axis of the constellation, as shown in Figure 12.14(c).[88]

The calculated values of phase and intensity can be represented, not only in a form of constellation diagram, but can also indicate the phasor trajectory, phase eye diagram, and demodulated output. This opens the possibility of measuring the imperfections in the signal driving the phase modulator,

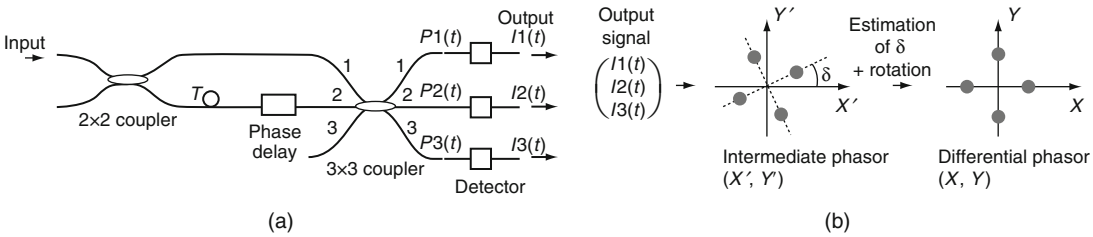

FIGURE 12.14

(a) Diagram of self-homodyne phasor monitor. (b) Symbol values obtained from monitor. (c) Constellation diagram after rotation through phasor-estimated phase.[88]

including the insufficient modulation depth or temporal skew between the arms of the modulator. These impairments are illustrated in Figures 12.15(a) and (b), respectively. In the case of multilevel phase-modulated signals, the phasor diagram enables precise adjustment of bias voltages in stacked MZM. Finally, the impairment due to ASE noise can be observed in the phasor diagram by measuring the ratio of the amplitude noise to the signal level. This enabled the monitoring of OSNR in range from 13 to 25 dB.

It ought to be mentioned that other examples of constellation diagram–based monitoring using self-homodyne detection have been presented in the literature. Monitoring of signal evolution and analysis of modulator adjustment have been demonstrated for both RZ-DQPSK[89] and RZ-8-APSK[90] modulations. These techniques use the modulated or unmodulated signal as a reference source and employ digital signal processing (DSP) for analysis and presentation of the acquired samples. Readers are referred to the respective articles for details of these techniques.

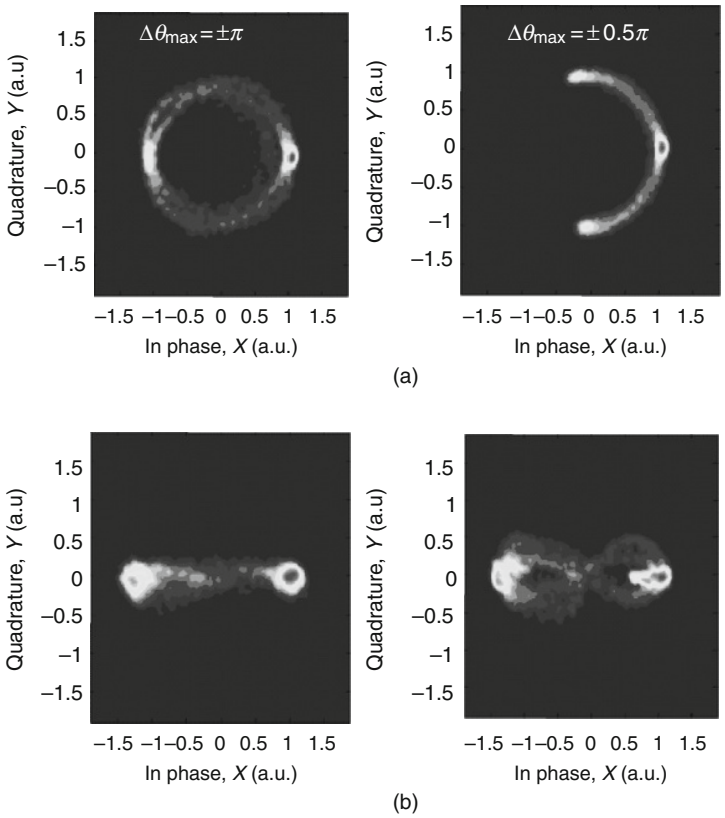

FIGURE 12.15

Constellation diagram obtained with differential phasor. (a) Phase modulation with driving voltage of V_Π and $1/2V_\Pi$. (b) PSK modulation without and with phase mismatch between arms of MZM.[88]

12.3.1.7 Asynchronous amplitude histogram

The monitoring techniques employing constellation diagrams provide ample information about the modulator characteristics and OSNR level affecting the signal. However, no methods employing the constellation diagrams to evaluate the influence of transmission impairments in phase-modulated channels have been presented to date. In order to obtain information about the level of CD or PMD affecting the signal, the samples need to be digitally processed. One of the methods to analyze the samples is to build a histogram of signal amplitude values. Such an approach is used to obtain a synchronous eye diagram, which can be used to extract information about signal noise, jitter, or waveform distortion. However, it requires a costly and format-dependent clock recovery circuit. A powerful OPM technique using asynchronous amplitude samples has been demonstrated for OOK signals.[91] The asynchronous amplitude histogram (AAH) OPM technique takes advantage of the statistical properties of the amplitude histogram to extract information about signal OSNR, accumulated CD, and PMD also in phase-modulated signals.[92–94] The AAH technique satisfies many of the requirements put on the OPM system. It is asynchronous and allows monitoring of multiple signal impairments.

The histogram is created by first sorting the samples by their value. The values are mapped onto histogram bins that uniformly divide the dynamic range of sample values into n levels. The histogram is formed by counting the number of amplitude samples falling into each of the bins and plotting the count as a function of the bin value. An example of an amplitude histogram for a 10-Gb/s RZ-DPSK signal is shown in Figure 12.16. The horizontal axis of the histogram represents the number of sample points in respective bins, while the vertical axis corresponds to the sample value. The peaks of the histogram correspond to the valley and the peak of signal waveform, respectively. The samples in between the peaks correspond to the crossover points of the rising and falling edge. In order to analyze the shape of the histogram, a distribution is fitted to each of the peaks. Histogram parameters reflect the properties of signal waveform. Therefore, by tracking the statistical properties of the histogram, it is possible to evaluate the level of impairments affecting the optical signal.

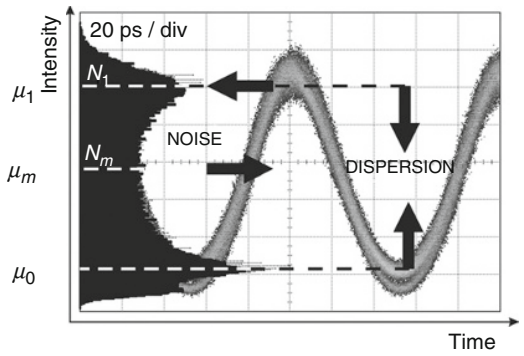

FIGURE 12.16

Waveform of RZ-DPSK signal and corresponding asynchronous amplitude histogram. Figure also shows parameters used for monitoring signal impairments.[92]

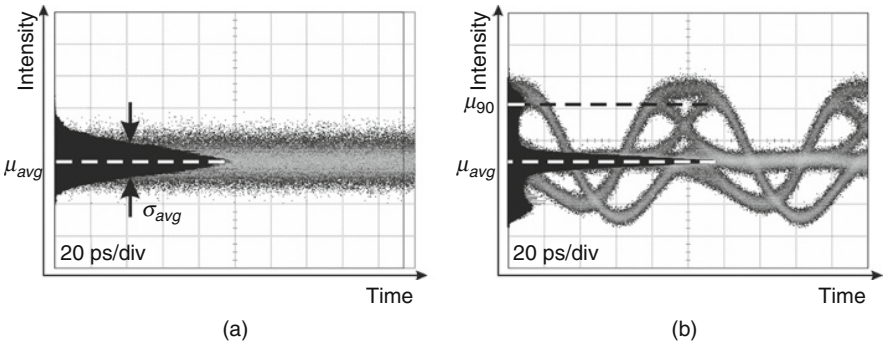

FIGURE 12.17

Waveform and the corresponding AAH for the NRZ-DPSK signals. (a) Parameter for monitoring OSNR. (b) Parameters for monitoring of CD.[92]

OSNR monitoring using AAH relies on dependence of the variance of signal-spontaneous beat noise on the power of ASE noise. In the case of an NRZ-DPSK signal generated by a phase modulator, the waveform is a constant-amplitude signal, as illustrated in Figure 12.17(a). The amplitude histogram acquired from the waveform consists of a single peak with mean value μ_{avg}. The fluctuation of waveform amplitude due to signal-spontaneous beat noise can be observed through the standard deviation σ_{avg} of histogram distribution, which is inversely proportional to the level of OSNR.

With this technique, the OSNR was evaluated from 22 to 38 dB in a 10-Gb/s NRZ-DPSK signal.[92] OSNR monitoring has also been demonstrated for RZ-DPSK and RZ-DQPSK formats. In this case, the histogram differs from that of the NRZ-DPSK waveform. It is comprised of two distribution peaks corresponding to the RZ pulse peak and the level of waveform valley between the pulses. OSNR reduction due to the change in ASE noise level causes a waveform fluctuation due to signal beating with ASE noise. Waveform fluctuation results in a reduced ratio between the histogram peak height and histogram height at median level, as shown in Figure 12.16. This phenomenon enables evaluation of the OSNR from 17 to 27 dB for the RZ-DPSK signal and from 17 to 30 dB for the RZ-DQPSK signal.[92] In this range the parameter scales linearly with the OSNR.

The AAH also serves to evaluate the level of residual CD affecting the signal. In the case of the NRZ-DPSK signal, the change of phase between bits introduces a frequency chirp proportional to the phase-modulator bandwidth. CD accumulation results in phase-to-amplitude conversion. This can be observed in the histogram that develops multiple peaks proportional to the conversion level. As CD does not influence the mean or standard deviation of the central histogram peak, it is possible to evaluate the accumulated CD level independently from the OSNR level. For a 10-Gb/s NRZ-DPSK, evaluation of CD is possible from -600 to $+600$ ps/nm.[92] The effect of CD accumulation in the RZ-DPSK or RZ-DQPSK signal can be observed in the waveform as spreading of pulses in time. This is reflected in the amplitude histogram, as shown in Figure 12.16. By measuring the distance between the peaks of the histogram, a parameter for evaluation of the accumulated CD can be established. CD monitoring for a 10-Gb/s RZ-DPSK signal and 20-Gb/s RZ-DQPSK signal was demonstrated from -600 to $+600$ ps/nm.[92] As the AAH reflects the statistical properties of waveform

amplitude, it is also sensitive to other transmission impairments, such as PMD. PMD monitoring has been demonstrated using the AAH for DGD up to 50 ps in the 10-Gb/s RZ-DPSK[94] and 20-Gb/s RZ-DQPSK[92] signals.

An alternative approach to monitoring the performance of phase-modulated signals using histogram analysis was presented in Reference 95. A self-clocked sampling module based on sum-frequency generation recovers a synchronized waveform of a demodulated channel. The samples forming the center of the obtained eye diagram are used for construction of the histogram. A Q-parameter is calculated from the statistical properties of the histogram and related to transmission impairments in 10-Gb/s RZ-DPSK and 40-Gb/s RZ-DQPSK signals.

12.3.1.8 Two-tap sampling

The asynchronous monitoring of transmission impairments in phase-modulated signals using amplitude histograms presented in the previous section reconstructs signal properties from individual intensity samples. This concept may be extended to the acquisition of sample pairs with a known relationship providing a reference in time or phase. A number of OPM techniques using sample pairs have been developed.

The principle of the delay-tap sampling technique, first demonstrated in Reference 96, is shown schematically in Figure 12.18(a). The OPM device input is the optical signal tapped from the transmission fiber. An optical BPF (OBPF) selects a single WDM channel for processing. The optical signal is split into two branches. One branch contains an optical delay line that introduces a time shift Δt between the optical signals. Subsequently, the light in both branches is converted into the electrical domain by a pair of photodiodes. Finally, the signals are fed into a sampling oscilloscope operating in X-Y mode. The voltage sampled in respective branches serves as X ($E(X)$) and Y ($E(Y)$) parameters in further analysis. The oscilloscope is operated by an external clock, independent of the monitored signal.

Simultaneous sampling of the electrical signal in two branches produces sample pairs. Effectively, this can be considered as sampling of the original waveform at two instants separated by the delay Δt. This is illustrated in Figure 12.18(b). The value of the delay shown in the figure is on the order of one-tenth of a symbol period. The exact choice of delay depends on which property of the signal is analyzed, as explained in the following paragraphs. The electrical signal samples at

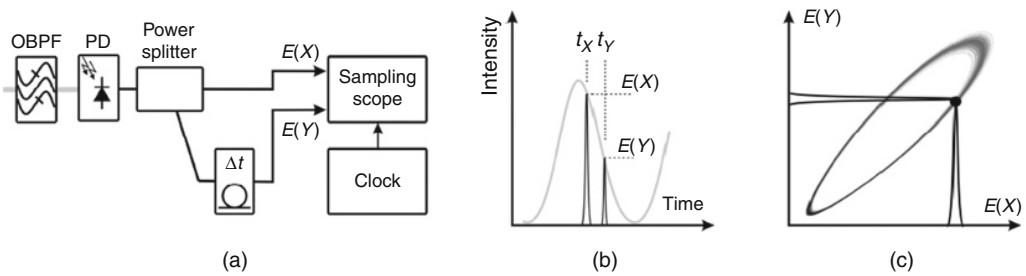

FIGURE 12.18

(a) Diagram of the monitor based on delay-tap sampling. (b) Acquisition of two samples with relative delay Δt. (c) Construction of delay-tap plot.[97]

times t_X and t_Y produce sample pairs with values $E(X)$ and $E(Y)$. The sample pairs are used to construct the delay-tap plot, as illustrated in Figure 12.18(c). Sample values serve as coordinates in the Cartesian system to plot individual points. The overlapping points from consecutive sampling instants form the delay-tap plot. This allows graphical decomposition of the waveform without synchronizing with the signal. The shape of the plot depends on the delay Δt and is influenced by changes in the signal waveform due to transmission impairments. Subsequent analysis of the delay-tap plot allows extraction of the information on the level of signal degradation.

In order to monitor OSNR degradation in the RZ-DPSK or RZ-DQPSK signal, a short delay Δt of one-tenth of a symbol period is used. The short delay between samples $E(X)$ and $E(Y)$ forms a narrow delay-tap plot that allows separation of the distributions of waveform peaks and valleys. The frequency of occurrence of sample pairs along the plot diagonal forms a histogram from which a noise parameter is calculated.[97] This parameter is similar but not equivalent to the synchronous Q-parameter due to the difference in statistical distribution of samples at the maximum eye opening captured by the synchronous sampling. Using the delay-tap plot analysis, the OSNR can be evaluated from 9 to 32 dB for the RZ-DPSK signal[97] and from 7 to 31 dB for the RZ-DQPSK signal.[98]

Monitoring the influence of residual CD on RZ-DPSK and RZ-DQPSK signals using the delay-tap plots relies on the waveform pulse carving and the relative phase of neighboring bits. The differential phase modulation conveys information in phase shifts between two consecutive symbols. For the RZ-DPSK signal, the possible phase shifts are 0 or π; for RZ-DQPSK, the possible phase shifts are 0, $\pm\pi/2$, or π. When an optical pulse is distorted by residual CD, it spreads beyond the allocated bit slot. The peak power of the pulse is reduced. Moreover, the shape of the waveform in between pulses is the result of interference between two neighboring bits and depends on the phase shift between the bits, as the constructive or destructive interference occurs. In order to track this phenomenon with the DTS technique, a 1-bit delay Δt, is employed. This allows comparing the waveforms of two neighboring bits. An algorithm based on the Hough transform is used to estimate accumulated CD from -600 to $+600$ ps/nm for both the 10-Gb/s RZ-DPSK[97] and 20-Gb/s RZ-DQPSK signals.[98] The delay-tap plot monitoring technique in conjunction with the Hough transform was also used to evaluate PMD for DGD of up to one-half a symbol period in the RZ-DQPSK signal. Alternatively, the analysis of the delay-tap plot using the Hausdorff distance for CD monitoring in NRZ-DPSK signals was presented in Reference 99. A different approach to delay-tap plot analysis was presented in Reference 100. The plots are formed using a fixed delay and the resulting images are analyzed using pattern recognition. This technique has been shown to be capable of evaluating impairment due to ASE noise, accumulated CD, and PMD.

The two-dimensional plots for monitoring optical impairments can also be constructed by sampling the constructive and destructive ports of the DI used for demodulation of the DPSK signal.[101] The two-tap plot is constructed by accumulating the samples with x values equal to the level of the signal in the destructive port and y values equal to the level of the signal in the constructive port, as shown in Figure 12.19. The analysis of the plot yields a Q-parameter that linearly increases with the conventional Q-parameter.

The concept of two-tap sampling has been extended to monitoring both the amplitude and phase of the NRZ-DPSK signal.[102] The field of the monitored channel is detected using a homodyne receiver. The signal is mixed with a local oscillator light in an optical hybrid and detected by two photodiodes. Two individual delay-tap plots are created for the phase and noise components, each with a delay of one-fifth of a symbol period. Analysis of the frequency histograms acquired along

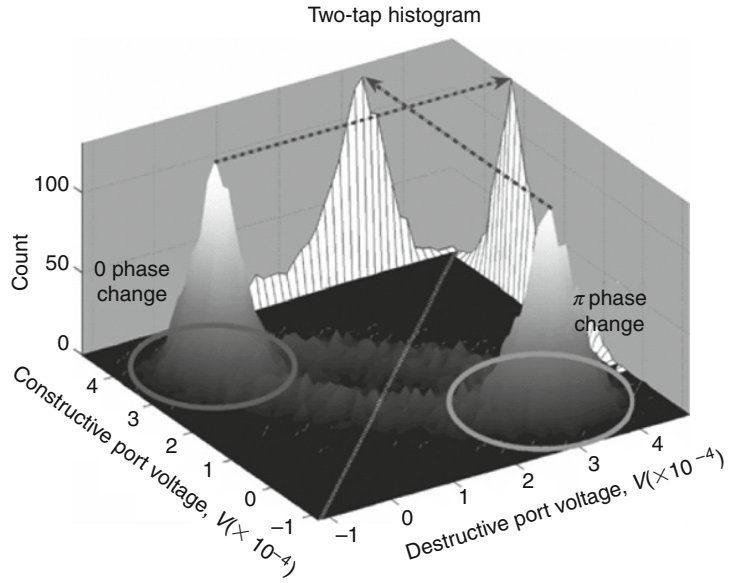

FIGURE 12.19

Two-tap plot constructed by sampling the constructive and destructive ports of the demodulator DI.[101]

the diagonal of each delay-tap plot enables estimation of transmission impairments. The delay-tap plot constructed from the amplitude component allows estimation of the OSNR from 10 to 30 dB, while the plot constructed from the phase component allows evaluation of accumulated CD from 0 to 750 ps/nm. OSNR and CD monitoring in a single channel is performed without a tunable optical filter, as the channel is separated by the frequency of the local oscillator.

12.3.1.9 Receiver-based monitoring

This section explains a group of OPM techniques that employ the optical receiver in order to analyze impairments in the phase-modulated signals.

A technique for monitoring the phase offset of the DQPSK demodulator from the center frequency of the signal is demonstrated in Reference 103. The technique employs a demodulator based on a 1-bit delay interferometer followed by a 90° hybrid and a pair of balanced photodiodes, as shown in Figure 12.20. The signal after the PD is limited to a value equal to the level obtained at the optimum phase of the demodulator. When a phase mismatch occurs, leading to the rotation of the constellation diagram with respect to the demodulator axes, the quadrature component that exceeds the limit is cropped, while the other component's power is reduced. Consequently, the average power of the monitor signal after the limiter drops while the phase mismatch between the modulator and the center frequency of the signal increases. Dithering of the phase offset in one of the arms of the demodulator allows reaching the optimum phase. Operation of this technique was proven experimentally for a 43-Gb/s RZ-DQPSK signal in the presence of accumulated CD of up to 250 ps/nm.

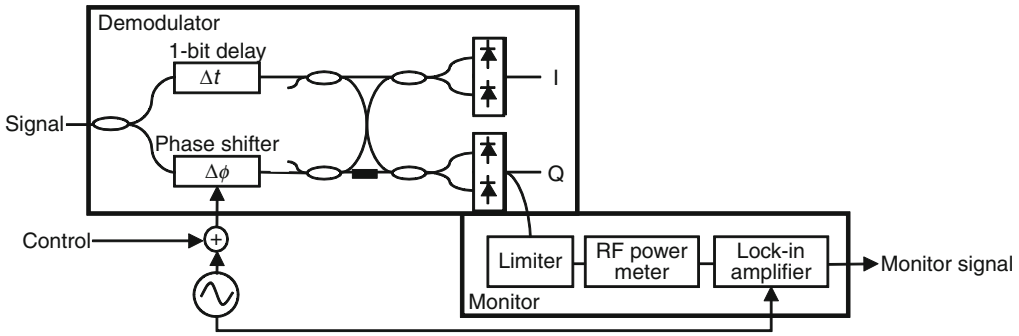

FIGURE 12.20

Diagram of phase-offset monitoring technique based on optical receiver and limiting amplifier.[103]

Finally, analysis of the synchronous eye diagram for monitoring a 40-Gb/s signal was demonstrated in Reference 104. The eye diagram received after the demodulator was analyzed using a neural network. The algorithm was trained with a set of signals affected by simulated impairments that enabled monitoring of OSNR, CD, and PMD. The evaluation range for the OSNR impairment was 18–30 dB, for the accumulated CD impairment from 7.5 to 52.5 ps/nm, and for PMD from 1.25 to 8.75 ps. This technique was also verified experimentally for monitoring impairments due to OSNR and CD.

12.3.2 Comparison of monitoring techniques

In order to realize OPM functionality, the presented techniques must fulfill a number of requirements. The desired characteristics of an OPM system are as follows:

- Transparency
- Asynchronous operation
- Multi-impairment monitoring
- Sensitivity
- Wide dynamic range
- Repeatability
- Affordable design

The concept of OPM transparency is in agreement with that of network transparency. This means flexibility in terms of signal bit rate and modulation format. On the other hand, transparency means that monitoring itself does not degrade the monitored signal. The requirement for asynchronous operation is one of the conditions for realizing transparent monitoring. The monitoring of multiple impairments is another important factor that should be satisfied by the monitoring equipment. A single technique should provide information about the degradations that are most likely to influence signal quality. The measurement or evaluation done through the OPM technique should be sensitive, have a wide dynamic range, and be repeatable. The dynamic range of the measurement defines the range of impairment values that the monitor is able to track, and it depends on the impairment type, signal bit rate, modulation format, and position of the device in the network.

Finally, repeatability or reliability of the measurement determines whether the parameter is uniformly evaluated when the impairment level remains constant. The last requirement of a successful OPM technique is affordable design. Although it is not directly related to the performance of the monitor, it plays an important role as the capital expenditures related to the deployment of the OPM equipment should be outweighed by the savings in operational expenditures. Therefore, affordable OPM techniques that provide a suitable range of measurement parameters are more likely to find their way into the realm of transparent networks. This section focuses on the comparison of OPM techniques for the phase-modulated signals from the perspective of general requirements for OPM equipment.

The techniques presented in this chapter may be arranged by the type of impairment that they are capable of monitoring. Such a comparison is presented in Figure 12.21. The center part of the figure lists the signal impairments described in Section 12.2.1. Impairments are linked to the techniques presented in Sections 12.3.1.2–12.3.1.9 that are capable of monitoring the respective impairments. The left side of the figure lists the spectrum-based monitoring techniques, while the right side presents the sampling-based techniques. It can be observed that most of the focus is concentrated on monitoring OSNR, CD, and PMD. Monitoring of NPN, power, Q-factor, and frequency offset receives less attention in the literature. Moreover, it may be observed that the sampling-based techniques are more versatile than the spectrum-based techniques. It must, however, be remembered that these techniques require high-speed components, such as broadband detectors and high-speed sampling.

The versatility of the monitoring techniques in terms of modulation format and impairment (including the evaluation range) are shown in Table 12.1. Measurement range values are recalculated for the 10-Gsymbol/s signals. Spectrum-based monitoring techniques provide wider ranges for monitoring impairments. Therefore, it may be concluded that the sampling-based techniques are more versatile, while requiring high-speed components, whereas the spectrum-based techniques should be chosen when the monitoring range is the priority.

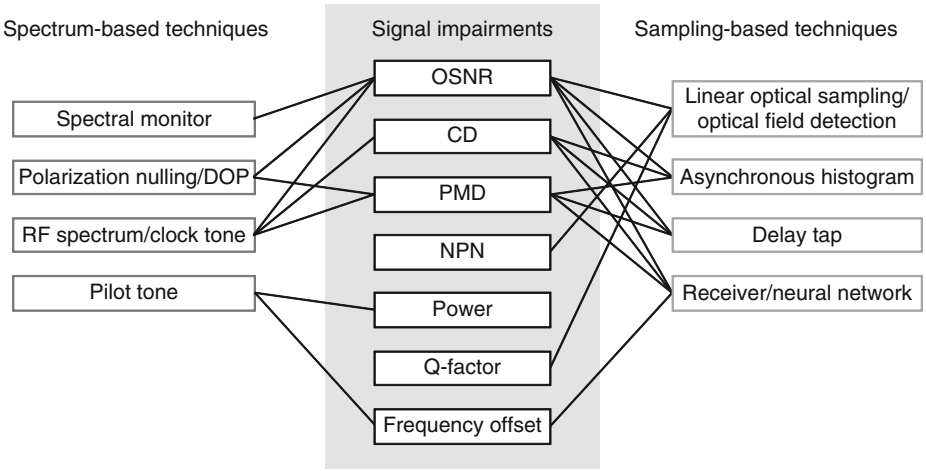

FIGURE 12.21

Analysis of OPM techniques by type of monitored impairment.

Table 12.1 Comparison of Measurement Ranges between OPM Techniques for Phase-Modulated Signals

Technique (references)	Format	Impairment	Range (for 10-Gsymbol/s signal)
Optical spectrum[64]	NRZ-DPSK	OSNR	0–28 (dB)
DOP[70]		OSNR	12–25 (dB)
DOP[71]	NRZ/RZ-DPSK	PMD	0–100 (ps)
DOP[72]	NRZ-DQPSK	PMD	0–100 (ps)
	RZ-DQPSK		0–50 (ps)
RF spectrum[76]	NRZ-DPSK	CD	0–800 (ps/nm)
RF spectrum[73]	RZ-DPSK	OSNR	15–35 (dB)
RF spectrum[74,75]	Pol-Mux RZ-DPSK	OSNR	11–29 (dB)
	Pol-Mux RZ-DPSK	PMD	0–48 (ps)
XPM[77]	RZ-D(Q)PSK	CD	0–1920 (ps/nm)
Clock tone[71,78]	NRZ-DPSK	CD	0–600 (ps/nm)
		PMD	0–50 (ps)
	RZ-DPSK	CD	0–900 (ps/nm)
Clock tone[72]	NRZ/RZ-DQPSK	CD	0–720 (ps/nm)
Pilot tone[79,83]	NRZ-DPSK	Offset	0∼±2 (0–±8[83]) (GHz)
AAH[92,93,94]		CD	0–600 (ps/nm)
	NRZ-DPSK	PMD	14–38 (dB)
	RZ-DPSK	OSNR	11–32 (dB)
	RZ-DQPSK		17–35 (dB)
DTS[99]	NRZ-DPSK	CD	0–400 (ps/nm)
DTS[97,98,99]		CD	0–600 (ps/nm)
		PMD	0–50 (ps)
	RZ-D(Q)PSK	OSNR	9–32 (dB)
DTS[100]		CD	0–850 (ps/nm)
DTS[101]	NRZ-DPSK	Q-factor	12–19 (dB)
Delay-tap optical field[102]	NRZ-DPSK	OSNR	10–30 (dB)
		CD	0–800 (ps/nm)
Receiver[103]	RZ-DQPSK	Offset	0–1.35 (GHz)
Neural network[104]	NRZ-DPSK	CD	0–640 (ps/nm)
		PMD	0–36 (ps)
		OSNR	18–30 (dB)

12.4 SUMMARY

This chapter discussed the most recent research in the OPM field for phase-modulated channels. Both the spectrum- and sampling-based techniques developed for the intensity-modulated channels have been adapted to accommodate the phase-modulated signals. In addition, new techniques

focusing on signal phase analysis have been introduced. By allowing the observation of transmission impairments directly in the optical layer, these techniques bring optical communication systems one step closer to transparent operation. It must, however, be remembered that the constant drive toward higher capacity leads to the introduction of more sophisticated modulation formats, covering more dimensions of modulation space, more levels of modulation, and higher symbol rates. These formats pose new challenges for OPM techniques as system tolerances become tighter and more sensitive parameters have to be employed. Therefore, it may be expected that OPM for phase-modulated signals will keep developing together with advances in transmission techniques.

ACKNOWLEDGMENTS

The author would like to thank Hidehiko Takara of NTT Network Innovation Laboratories, as well as Ken-ichi Kitayama and Akihiro Maruta of Osaka University for valuable discussions.

REFERENCES

1. O'Mahony MJ, Politi C, Klonidis D, Nejabati R, Simeonidou D. Future optical networks. *J Lightwave Technol* 2006;**24**:4684–96.
2. Gladisch A, Braun RP, Breuer D, Ehrhardt A, Foisel HM, Jaeger M, et al. Evolution of terrestrial optical system and core network architecture. *Proc. IEEE* 2006;**94**:869–91.
3. Winzer P, Essiambre RJ. Advanced optical modulation formats. *Proc. IEEE* 2006;**94**:952–85.
4. Miyamoto Y. Advanced modulation formats for high-capacity optical transport network. In: *Proc. 31st European conference on optical communication (ECOC) 2005*, Glasgow, Scotland, vol. 4, p. 777–80; 2005.
5. Mizuochi T. Recent progress in forward error correction and its interplay with transmission impairments. *IEEE J Sel Top Quantum Electron* 2006;**12**:544–54.
6. Xu C, Liu X, Wei X. Differential phase-shift keying for high spectral efficiency optical transmissions. *IEEE J Sel Top Quantum Electron* 2004;**10**:281–93.
7. Charlet G. Progress in optical modulation formats for high-bit rate WDM transmissions. *IEEE J Sel Top Quantum Electron* 2006;**12**:469–83.
8. Gnauck A, Winzer P. Optical phase-shift-keyed transmission. *J Lightwave Technol* 2005;**23**:115–30.
9. Xie C, Moller L, Haunstein H, Hunsche S. Comparison of system tolerance to polarization-mode dispersion between different modulation formats. *IEEE Photon Technol Lett* 2003;**15**:1168–70.
10. Vassilieva O, Hoshida T, Choudhary S, Castanon G, Kuwahara H, Terahara T, et al. Numerical comparison of NRZ, CS-RZ and IM-DPSK formats in 43 Gbit/s WDM transmission. In: *Proc. LEOS 2001*, San Diego, CA, vol. 2, p. 673–74; 2001.
11. Miyano T, Fukutoku M, Hattori K, Ono H. Suppression of degradation induced by SPM/XPM + GVD in WDM transmission using a bit-synchronous intensity modulated DPSK signal. In: *Proc. OECC 2000*, Chiba, Japan, p. 580–81; 2000.
12. Cho PS, Khurgin JB. Suppression of cross-gain modulation in SOA using RZ-DPSK modulation format. *IEEE Photon Technol Lett* 2003;**15**:162–4.
13. Hirano A, Miyamoto Y. Novel modulation formats in ultra-high-speed transmission systems, and their applications. In: *Proc. OFC 2004*, Los Angeles, CA, paper ThM1. 2004.
14. Zhu B, Nelson LE, Stulz S, Gnauck AH, Doerr C, Leuthold J, et al. High spectral density long-haul 40-Gb/s transmission using CSRZ-DPSK format. *J Lightwave Technol* 2004;**22**:208–14.

15. Zhu B, Nelson LE, Stulz S, Gnauck AH, Doerr C, Leuthold J, et al. 6.4 Tb/s (160 × 42.7 Gb/s) transmission with 0.8 bit/s/Hz spectral efficiency over 32 × 100 km of fiber using CSRZ-DPSK format. In: *Proc. OFC 2003*, Atlanta, GA, paper PD19. 2003.
16. Wree C, Leibrich J, Eick J, Rosenkranz W, Mohr D. Experimental investigation of receiver sensitivity of RZ-DQPSK modulation using balanced detection. In: *Proc. OFC 2003*, Atlanta, GA, paper ThE5. 2003.
17. Ohm M, Speidel J. Quaternary optical ASK-DPSK and receivers with direct detection. *IEEE Photon Technol Lett* 2003;**15**:159–61.
18. Yadin Y, Orenstein M, Shtaif M. Optical DPASK and DQPSK: a comparative analysis for linear and nonlinear transmission. *IEEE J Sel Top Quantum Electron* 2006;**12**:581–8.
19. Winzer PJ, Essiambre R-J. Advanced optical modulation formats. In: Kaminow IP, Li T, Willner AE, editors. *Optical fiber telecommunications V B: Systems and Networks*. New York: Academic Press; 2008.
20. Sekine K, Kikuchi N, Mandai K, Sasaki S. Advanced multi-level transmission systems. In: *Proc. OFC 2008*, San Diego, CA, paper OMI4. 2008.
21. Serbay M, Wree C, Rosenkranz W. Experimental investigation of RZ-8DPSK at 3×10.7 Gb/s. In: *Proc. LEOS 2005*, Sydney, Australia, p. 483–84; 2005.
22. Nazarathy M, Simony E. Performance limits of multilevel DPSK. *IEEE Photon Technol Lett* 2005;**17**:2310–2.
23. Agrawal GP. *Fiber-optic communication systems. Wiley series in microwave and optical engineering*, 3rd ed. New York: John Wiley & Sons, Inc.; 2002.
24. Winzer P, Chandrasekhar S, Kim H. Impact of filtering on RZ-DPSK reception. *IEEE Photon Technol Lett* 2003;**15**:840–2.
25. Bosco G, Poggiolini P. On the Q factor inaccuracy in the performance analysis of optical direct-detection DPSK systems. *IEEE Photon Technol Lett* 2004;**16**:665–7.
26. Boffi P, Marazzi L, Paradiso L, Parolari P, Righetti A, Siano R, et al. Experimental comparison of RZ-IMDD and RZ-DQPSK performance in a standard 2000-km DWDM system. In: *Proc. CLEO 2004*, San Francisco, CA, paper CThBB5. 2004.
27. Gnauck A, Winzer P, Dorrer C, Chandrasekhar S. Linear and nonlinear performance of 42.7-Gb/s single-polarization RZ-DQPSK format. *IEEE Photon Technol Lett* 2006;**18**:883–5.
28. Sinsky J, Adamiecki A, Gnauck A, Burrus C, Leuthold J, Wohlgemuth O, et al. RZ-DPSK transmission using a 42.7-Gb/s integrated balanced optical front end with record sensitivity. *J Lightwave Technol* 2004;**22**:180–5.
29. Willner A, Nezam S, Yan L, Pan Z, Hauer M. Monitoring and control of polarization-related impairments in optical fiber systems. *J Lightwave Technol* 2004;**22**:106–25.
30. Kim H, Doerr C, Pafchek R, Stulz L, Bernasconi P. Polarisation-mode dispersion impairments in direct-detection differential phase-shift-keying systems. *Electron Lett* 2002;**38**:1047–8.
31. Wang J, Kahn JM. Impact of chromatic and polarization-mode dispersions on DPSK systems using interferometric demodulation and direct detection. *J Lightwave Technol* 2004;**22**:362–71.
32. Chandrasekhar S, Liu X. Experimental investigation of system impairments in polarization multiplexed 107-Gb/s RZ-DQPSK. In: *Proc. OFC 2008*, San Diego, CA, paper OThU7. 2008.
33. Kim H, Winzer P. Robustness to laser frequency offset in direct-detection DPSK and DQPSK systems. *J Lightwave Technol* 2003;**21**:1887–91.
34. Gene J, Soler M, Killey R, Prat J. Investigation of 10-Gb/s optical DQPSK systems in presence of chromatic dispersion, fiber nonlinearities, and phase noise. *IEEE Photon Technol Lett* 2004;**16**:924–6.
35. Freund R, Seimetz M. Higher order modulation formats using coherent detection and electronic distortion equalisation for application in future backbone networks. In: *Proc. IEEE/LEOS 2008*, Newport Beach, CA, paper WD3.3. 2008.
36. Gnauck A. 40-Gb/s RZ-differential phase shift keyed transmission. In: *Proc. OFC 2003*, Atlanta, GA, p. 450–51; 2003.

37. Wree C, Leibrich J, Rosenkranz W. RZ-DQPSK format with high spectral efficiency and high robustness towards fiber nonlinearities. In: *Proc. ECOC 2002*, Copenhagen, Denmark, paper 9.6.6. 2002.
38. Gordon P, Mollenauer LF. Phase noise in photonic communications systems using linear amplifiers. *Optics Lett* 1990;**15**:1351–3.
39. Xu C, Liu X, Mollenauer LF, Wei X. Comparison of return-to-zero differential phase-shift keying and ON-OFF keying in long-haul dispersion managed transmission. *IEEE Photon Technol Lett* 2003;**15**:617–9.
40. Kim H. Cross-phase-modulation-induced nonlinear phase noise in WDM direct-detection DPSK systems. *J Lightwave Technol* 2003;**21**:1770–4.
41. Kim H, Gnauck A. Experimental investigation of the performance limitation of DPSK systems due to nonlinear phase noise. *IEEE Photon Technol Lett* 2003;**15**:320–2.
42. Ho KP. Performance degradation of phase-modulated systems due to nonlinear phase noise. *IEEE Photon Technol Lett* 2003;**15**:1213–5.
43. Liu X. Nonlinear effects in phase shift keyed transmission. In: *Proc. OFC 2004*, Los Angeles, CA, paper ThM4. 2004.
44. Boffi P, Marazzi L, Paradiso L, Parolari P, Righetti A, Setti D, et al. 20 Gb/s differential quadrature phase-shift keying transmission over 2000 km in a 64-channel WDM system. *Opt Commun* 2004;**237**:319–23.
45. Wen YJ, Nirmalathas A, Lee DS. RZ/CSRZ-DPSK and chirped NRZ signal generation using a single-stage dual-electrode Mach-Zehnder modulator. *IEEE Photon Technol Lett* 2004;**16**:1041–135.
46. Ohm M, Freckmann T. Comparison of different DQPSK transmitters with NRZ and RZ impulse shaping. In: *Proc. IEEE/LEOS workshop on advanced modulation formats*, Rio Grande, Puerto Rico, paper ThB2. ; 2004.
47. Ho KP, Cuei HW. Generation of arbitrary quadrature signals using one dual-drive modulator. *J Lightwave Technol* 2005;**23**:764–70.
48. Griffin RA, Carter AC. Optical differential quadrature phase-shift key (oDQPSK) for high capacity optical transmission. In: *Proc. OFC 2002,* Anaheim, CA, paper WX6. 2002.
49. Bosco G, Poggiolini P. Analysis of impact of receiver imperfections on performance of optical DQPSK systems. *Electron Lett* 2004;**40**:1147–9.
50. Bosco G, Poggiolini P. On the joint effect of receiver impairments on direct-detection DQPSK systems. *J Lightwave Technol* 2006;**24**:1323–33.
51. Kilper DC, Bach R, Blumenthal D, Einstein D, Landolsi T, Ostar L, et al. Optical performance monitoring. *J Lightwave Technol* 2004;**22**:294–304.
52. Weingartner W, Kilper DC. OSNR monitoring for fault management in high speed networks. In: *Proc. ECOC 2002*, Copenhagen, Denmark, paper 7.4.5. 2002.
53. Kilper DC, Weingartner W. Monitoring optical network performance degradation due to amplifier noise. *J Lightwave Technol* 2003;**21**:1171–8.
54. Willner AE, Pan Z, Yu C. Optical performance monitoring. In: Kaminow IP, Li T, Willner AE, editors. *Optical fiber telecommunications V B: systems and networks*. New York: Academic Press; 2008.
55. Xu C, Liu X. Postnonlinearity compensation with data-driven phase modulators in phase-shift keying transmission. *Electron Lett* 2002;**27**:1619–21.
56. Hansryd J, van Howe J, Xu C. Experimental demonstration of nonlinear phase jitter compensation in DPSK modulated fiber links. *IEEE Photon Technol Lett* 2005;**17**:232–4.
57. Zhu G, Mollenauer L, Xu C. Experimental demonstration of postnonlinearity compensation in a multispan DPSK transmission. *IEEE Photon Technol Lett* 2006;**18**:1007–9.
58. Liu X, Wei X, Slusher RE, McKinstrie CJ. Improving transmission performance in differential phase-shift-keyed systems by use of lumped nonlinear phase-shift compensation. *Optics Lett* 2002;**27**:1616–8.
59. Matsumoto M, Kamio T. Nonlinear phase noise reduction of DQPSK signals by a phase-preserving amplitude limiter using four-wave mixing in fiber. *IEEE J Sel Top Quantum Electron* 2008;**14**:610–5.
60. Ho KP, Kahn JM. Electronic compensation technique to mitigate nonlinear phase noise. *J Lightwave Technol* 2004;**22**:779–83.

61. Kikuchi K. Electronic post-compensation for nonlinear phase fluctuations in a 1000-km 20-Gbit/s optical quadrature phase-shift keying transmission system using the digital coherent receiver. *Opt Express* 2008;**16**:889–96.
62. ITU-T. *Optical monitoring for DWDM systems*. ITU-T G.697. 2004.
63. Kilper DC, Chandrasekhar S, Buhl L, Agarwal A, Maywar D. Spectral monitoring of OSNR in high-speed networks. In: *Proc. ECOC 2002*, Copenhagen, Denmark, paper 7.4.4. 2002.
64. Jeon SW, Kim YH, Lee BH, Jung MA, Park CS. OSNR monitoring technique based on cascaded long-period fiber grating with optically tunable phase shifter. *Opt Express* 2008;**16**:20603–9.
65. Liu X, Kao YH, Chandrasekhar S, Kang I, Cabot S, Buhl LL. OSNR monitoring method for OOK and DPSK based on optical delay interferometer. *IEEE Photon Technol Lett* 2007;**19**:1172–4.
66. Lee J, Jung D, Kim C, Chung Y. OSNR monitoring technique using polarization-nulling method. *IEEE Photon Technol Lett* 2004;**13**:88–90.
67. Lee JH, Choi HY, Shin SK, Chung YC. A review of the polarization-nulling technique for monitoring optical-signal-to-noise ratio in dynamic WDM networks. *J Lightwave Technol* 2006;**24**:4162–71.
68. Moench W, Larikova J. Measuring the optical signal-to-noise ratio in agile optical networks. In: *Proc. OFC 2007*, Anaheim, CA, paper NWC1. 2007.
69. Skold M, Olsson B-E, Sunnerud H, Karlsson M. PMD-insensitive DOP-based OSNR monitoring by spectral SOP measurements. In: *Proc. OFC 2005,* Anaheim, CA, paper NWC1. 2007.
70. Lu GW, Cheung MH, Chen LK, Chan CK. Simple PMD-insensitive OSNR monitoring scheme assisted by transmitter-side polarization scrambling. *Opt Express* 2006;**14**:58–62.
71. Pan Z, Wang Y, Song Y, Motaghian R, Havstad S, Willner A. Monitoring chromatic dispersion and PMD impairments in optical differential phase-shift-keyed (DPSK) systems. In: *Proc. OFC 2003*, Atlanta GA, p. 402–3; 2003.
72. Wang Y, Hu S, Yan L, Yang JY, Willner AE. Chromatic dispersion and polarization mode dispersion monitoring for multi-level intensity and phase modulation systems. *Opt Express* 2007;**15**:14038–43.
73. Dorrer C, Liu X. Noise monitoring of optical signals using RF spectrum analysis and its application to phase-shift-keyed signals. *IEEE Photon Technol Lett* 2004;**16**:1781–3.
74. Yang JY, Zhang L, Yue Y, Arbab VR, Agarwal A, Paraschis L, et al. Optical signal-to-noise ratio monitoring of an 80 Gbits/s polarization-multiplexed return-to-zero differential phase-shift keying channel. *Optics Lett* 2009;**34**:1006–8.
75. Yang J-Y, Zhang L, Yue Y, Christen LC, Zhang B, Jackel J, et al. CD-insensitive PMD monitoring of an 80-Gb/s polarization-multiplexed RZ-DPSK channel using a polarizer and a low-speed detector. In: *Proc. OFC 2009,* San Diego, CA, paper OThJ2. 2009.
76. Zhao J, Qureshi KK, Li ZH, Lu C, Tam HY, Wai PKA. Chromatic dispersion monitoring of DPSK signals using RF power detection. In: *Proc. SPIE 7136*, paper 71361H. 2008.
77. Yang J-Y, Zhang L, Wu T, Wu X, Christen LC, Nuccio S, et al. Chromatic dispersion monitoring of 40-Gb/s RZ-DPSK and 80-Gb/s RZ-DQPSK data using cross-phase modulation in highly-nonlinear fiber and a simple power monitor. In: *Proc. OFC 2008*, San Diego, CA, paper OTuG5. 2008.
78. Lize YK, Christen L, Yang JY, Saghari P, Nuccio S, Willner AE, et al. Independent and simultaneous monitoring of chromatic and polarization-mode dispersion in OOK and DPSK transmission. *IEEE Photon Technol Lett* 2007;**19**:3–5.
79. Ji HC, Park KJ, Lee JH, Chung HS, Son ES, Han KH, et al. Optical performance monitoring techniques based on pilot tones for WDM network applications. *J Opt Netw* 2004;**3**:510–33.
80. Park KJ, Ji HC, Chung YC. Optical channel monitoring technique using phase-modulated pilot tones. *IEEE Photon Technol Lett* 2005;**17**:2481–3.
81. Jun S, Kim H, Park P, Lee J, Chung Y. Pilot-tone-based WDM monitoring technique for DPSK systems. *IEEE Photon Technol Lett* 2006;**18**:2171–3.
82. Ji HC, Park PKJ, Kim H, Lee JH, Chung YC. A novel frequency-offset monitoring technique for direct-detection DPSK systems. *IEEE Photon Technol Lett* 2006;**18**:950–2.

83. Christen L, Nuccio S, Lize YK, Jayachandran N, Willner AE, Paraschis L. Stabilization of a 40 Gb/s DPSK delay-line interferometer using half bit-rate AM pilot tone monitoring. In: *Proc. CLEO 2007*, Baltimore, MD, paper CMJJ2. 2007.
84. Andrekson P. High resolution optical waveform and eye diagram monitoring. In: *Proc. OFC 2007*, Anaheim, CA, paper OThN3. 2007.
85. Dorrer C, Doerr CR, Kang I, Ryf R, Leuthold J, Winzer PJ. Measurement of eye diagrams and constellation diagrams of optical sources using linear optics and waveguide technology. *J Lightwave Technol* 2005;**23**:178–86.
86. Dorrer C. Monitoring of optical signals from constellation diagrams measured with linear optical sampling. *J Lightwave Technol* 2006;**24**:313–21.
87. Dorrer C, Gnauck AH, Winzer PJ, Chandrasekhar S. Investigation of 42.7-Gb/s quadrature phase-shift keying (QPSK) signals using linear optical sampling. In: *Proc. CLEO 2005*, Baltimore, MD, paper CMHH4. 2005.
88. Takushima Y, Choi HY, Chung YC. Monitoring techniques for phase and OSNR of DPSK/DQPSK signals. In: *Proc. SPIE 2008*, paper 71360U. 2008.
89. Tanimura K, Ohta H. Monitoring of DPSK/DQPSK signals using 1-bit delayed self-homodyne detection with optical phase diversity. In: *Proc. ECOC 2007*, Berlin, Germany, paper P065. 2007.
90. Kikuchi N, Sekine K, Sasaki S. Time-resolved waveform measurement of high-speed phase-modulated optical signals using self-homodyne interferometry. In: *Proc. ECOC 2005*, Glasgow, Scotland, p. 391–92; 2005.
91. Shake I, Takara H. Averaged Q-factor method using amplitude histogram evaluation for transparent monitoring of optical signal-to-noise ratio degradation in optical transmission system. *J Lightwave Technol* 2002;**20**:1367–73.
92. Kozicki B, Ohara T, Takara H. Optical performance monitoring of phase-modulated signals using asynchronous amplitude histogram analysis. *J Lightwave Technol* 2008;**26**:1353–61.
93. Li Z, Lu C, Wang Y, Li G. In-service signal quality monitoring and multi-impairment discrimination based on asynchronous amplitude histogram evaluation for NRZ-DPSK systems. *IEEE Photon Technol Lett* 2005;**17**:1998–2000.
94. Li Z, Li G. Chromatic dispersion and polarization-mode dispersion monitoring for RZ-DPSK signals based on asynchronous amplitude-histogram evaluation. *J Lightwave Technol* 2006;**24**:2859–66.
95. Yoshikane N, Tsuritani T, Lee JH, Otani T. All-optical performance monitoring of multi-bitrate and multi-format signals based on optical sampling for transparent optical networks. In: *Proc. SPIE 2008*, paper 713637. 2008.
96. Anderson TB, Dods SD, Wong E, Farrell PM. Asynchronous measurement of chromatic dispersion from waveform distortion. In: *Proc. OFC 2006*, Anaheim, CA, paper OWN4. 2006.
97. Kozicki B, Maruta A, Kitayama K. Experimental demonstration of optical performance monitoring for RZ-DPSK signals using delay-tap sampling method. *Opt Express* 2008;**16**:3566–76.
98. Kozicki B, Maruta A, Kitayama KI. Experimental investigation of delay-tap sampling technique for online monitoring of RZ-DQPSK signals. *IEEE Photon Technol Lett* 2009;**21**:179–81.
99. Zhao J, Lu C, Lam KM, Li ZH, Tam HY, Wai PK. A novel optical signal monitoring method of DPSK signal based on delay tap sampling and Hausdorff distance measure. In: *Proc. CLEO/QELS 2008*, San Jose, CA, paper JWA108. 2008.
100. Clarke K, Anderson T, Dods S. Monitoring of multiple modulation formats using asynchronous delay-tap sampling. In: *Proc. COIN-ACOFT 2007*, Melbourne, Australia, paper MoA1–2. 2007.
101. Jong KC, Tsao HW, Lee SL. Q-factor monitoring of optical signal-to-noise ratio degradation in optical DPSK transmission. *Electron Lett* 2008;**44**:761–3.
102. Choi HY, Takushima Y, Chung YC. Multiple-impairment monitoring technique using optical field detection and asynchronous delay-tap sampling method. In: *Proc. OFC 2009*, San Diego, CA, paper OThJ5. 2009.
103. Kawakami H, Yoshida E, Miyamoto Y, Oguma M, Itoh T. Simple phase offset monitoring technique for 43 Gbit/s optical DQPSK receiver. *Electron Lett* 2008;**44**:437–8.
104. Wu X, Jargon J, Willner AE. Off-line monitoring of OSNR/CD/PMD degradation effects using neural-network-based training sequences. In: *Proc. ECOC 2008*, Brussels, Belgium, paper We 3.D.6. ; 2008.